October 2021

Visuomotor Adaptation During Asymmetric Walking

Charles Napoli
University of Massachusetts Amherst

VISUOMOTOR ADAPTATION DURING ASYMMETRIC WALKING

A Thesis Presented

by

CHARLES D. NAPOLI

Submitted to the Graduate School of the

University of Massachusetts Amherst in fulfillment

of the requirements for the degree of

MASTER OF SCIENCE

September 2021

Department of Kinesiology

VISUOMOTOR ADAPTATION DURING ASYMMETRIC WALKING

A Thesis Presented

By

CHARLES D. NAPOLI

Approved as to style and content by:

_____
Richard E.A. van Emmerik, Chair

_____
Joseph Hamill, Member

_____
Wouter Hoogkamer, Member

_____
Richard E.A. van Emmerik, Department Head
Department of Kinesiology

ABSTRACT

VISUOMOTOR ADAPTATION DURING ASYMMETRIC WALKING

SEPTEMBER 2021

CHARLES D. NAPOLI, B.S., UNIVERSITY OF MASSACHUSETTS AMHERST

M.S., UNVIERSITY OF MASSACHUSETTS AMHERST

Directed by: Richard van Emmerik

Necessary for effective ambulation, head stability affords optimal conditions for the perception of visual information during dynamic tasks. This maintenance of head-in-space equilibrium is achieved, in part, by the attenuation of the high frequency impact shock resulting from ground contact. While a great deal of experimentation has been done on the matter during steady state locomotion, little is known about how head stability or dynamic visual acuity is maintained during asymmetric walking.

In this study, fifteen participants were instructed to walk on a split-belt treadmill for ten minutes while verbally reporting the orientation of a randomized Landolt-C optotype that was projected at heel strike. Participants were exposed to the baseline, adaptation, and washout conditions, as characterized by belt speed ratios of 1:1, 1:3, and 1:1, respectively. Step length asymmetry, shock attenuation, high (impact) and low (active) frequency head signal power, and dynamic visual acuity scores were averaged across the first and last fifty strides of each condition.

Over the course of the first fifty strides, step length asymmetry was significantly greater during adaptation than during baseline (p <0.001; d =2.442). Additionally, high frequency head signal power was significantly greater during adaptation than during baseline (p <0.001; d =1.227), indicating a reduction in head stability. Shock attenuation was significantly lower during adaptation than during baseline (p <0.05; d =-0.679), and a medium effect size suggests that dynamic visual acuity was lower

during adaptation than during baseline as well (p =0.052; d =0.653). When comparing the baseline and adaptation conditions across the last fifty strides, however, many of these decrements were greatly reduced.

The results of this study indicate that the locomotor asymmetry imposed by the split-belt treadmill during the early adaptation condition is responsible for moderate decrements to shock attenuation, head stability, and dynamic visual acuity. Moreover, the relative reduction in magnitude of these decrements across the last fifty strides underscores the adaptive nature of the locomotor and visuomotor systems.

Table of Contents

LIST OF FIGURES

LIST OF TABLES

Page

LIST OF EQUATIONS

Page

CHAPTER 1
INTRODUCTION

1.1 Background

The human system has evolved the capacity to interact with its environment in a manner that is both stable and adaptable, despite the dynamic nature of the environment with which it interacts. Necessary to this interaction is the perception of environmental information such that it informs the actions taken by the system, which in-turn alter the state of the environment (Gibson, 1986). There is perhaps no greater evidence of this necessity than the intricacies of the visuomotor system. The vestibulo-ocular reflex, for example, is composed of elaborate neuronal networks dedicated to the integration of the vestibular system and the ocular muscles (Leigh & Zee, 2015). This integration allows the visuomotor system to mitigate any perturbing effects that head movement might have on visual field stability, thereby aiding in the perception of visual information (Leigh et al., 2015). Similarly, the vestibulo-collic reflex integrates the vestibular system and the neck musculature responsible for stabilizing the head, thus allowing for improved visual field stability and, by extension, improved visual acuity (Wilson et al., n.d.).

While the reflexes described above are necessary to the maintenance of visual field stability, they are ultimately insufficient in their contributions to dynamic visual acuity. Indeed, the perception of visual information during dynamic tasks requires the coordination of the visual, vestibular, and locomotor systems, despite each of these systems acting upon their own distinctive sources of environmental information. The visual system, by definition, acts upon visual information; the vestibular system acts upon inertial information; and the integration of the two gives rise to phenomena such as the vestibulo-ocular reflex (Leigh et al., 2015). The locomotor system, however, is unique in its information source. Bipedal locomotion requires that visual, vestibular, mechanical, and proprioceptive information sources are integrated continuously while informing both volitional and reflexive control

strategies. The integration of these information sources permits the locomotor system to adaptively respond to ecological constraints, thus aiding in the execution of complex tasks such as visual perception during locomotion.

During locomotion, the deceleration of the musculoskeletal system following ground-contact results in a shockwave that is transmitted towards the head, potentially disrupting the stability of the visual field (Hamill, Derrick, & Holt, 1995). Accordingly, the locomotor system must adaptively attenuate this shockwave as to afford optimal conditions for the function of the visual and vestibular systems. The attenuation of this shockwave results from the ability of the locomotor system to act as a low-pass filter, absorbing high frequency accelerations through the deformation of passive (e.g., bones and tendons) and active structures (e.g., skeletal muscle) (Pulaski, Zee, & Robinson, 1981a). The adaptive nature by which the locomotor system affords a consistent basis for visuomotor function was underscored in work by Hamill et al., which measured head and tibia accelerations across a number of stride frequencies. While high stride frequencies were associated with low tibial accelerations and low stride frequencies were associated with high tibial accelerations, accelerations at the head were found to remain relatively constant across all conditions. By adaptively modulating the amount of energy absorbed by passive and active structures during locomotion, the system is able to maintain head stability, thereby facilitating optimal conditions for visual perception (Hamill et al., 1995).

Given the complexity of the locomotor system, a number of experimental paradigms have been employed in an effort to better understand how locomotor adaptation might occur under various conditions. Of these paradigms, the one with greatest relevance to this paper is that of the split-belt adaptation paradigm, in which participants are exposed to a treadmill with two independent belts capable of moving at different speeds (Dietz, Zijlstra, & Duysens, 1994). Upon initial exposure to this perturbation, healthy participants experience decrements to interlimb coordination and exhibit asymmetrical gait. As exposure continues, the locomotor system adapts, and gait parameters shift

towards baseline symmetry (Dietz et al., 1994). When the treadmill is returned to its tied-belt function where both belts are moving at the same speed, participants experience a loss of symmetry mirroring that which occurs during initial exposure to the split-belt condition. These periods of adaptation and deadaptation suggest the occurrence of motor learning in which ecological constraints (e.g., imposed asymmetry) are perceived and subsequently stored by the locomotor system (Roemmich & Bastian, 2018).

While independent measures of shock attenuation and gait symmetry are useful in the study of locomotor adaptation, neither of these measures directly assess the capacity of the system to dynamically perceive visual information. Dynamic visual acuity, then, is typically measured by having participants report the perceived orientations of optotypes (e.g., Landolt-C) during dynamic tasks such as walking or running (Peters & Bloomberg, 2005). As visual perception requires the coordination of the visual, vestibular, and locomotor systems, a direct measure of dynamic visual acuity may prove useful in exposing any changes in performance to any of the above systems. Likewise, by measuring shock attenuation and gait symmetry during a visual task while participants are exposed to a perturbing environment, the underlying contributions of locomotor adaptation to visual perception might be exposed.

1.2 Statement of the Problem

Necessary for effective ambulation, head stability affords optimal conditions for the perception of visual information during dynamic tasks. The adaptive capacity of the locomotor system contributes to head stability primarily by modulating the energy absorbed by active structures (e.g., skeletal muscle). While prior work has examined both shock attenuation and dynamic visual acuity during normal locomotion, little is known about the mechanisms underlying head stability and visual perception during asymmetrical gait. By examining dynamic visual acuity performance and head stability

as functions of gait asymmetry, a better understanding of the relationship between the locomotor and visuomotor systems might be achieved.

1.3 Purpose of the Study and its Significance

This study aims to investigate the relationship between locomotor asymmetry and visual field stability through the combination of several well established yet disparate experimental paradigms. By assessing head stability and dynamic visual acuity throughout the split-belt adaptation, the coordinative strategies leading to visuomotor adaptation and improved visual perception might be exposed. Doing so will serve to advance neurorehabilitation strategies for those with deficits to the locomotor and visuomotor systems by providing an improved understanding of how these two systems interact.

1.4 Specific Aims

The proposed study aims to answer three fundamental questions on the relationship between locomotor asymmetry, head stability, visual perception, and motor learning. Answering these questions should serve to further our understanding of how the locomotor and visuomotor systems interact in response to ecological constraints (e.g., imposed locomotor asymmetry).

Aim 1 *will examine the relationship between locomotor asymmetry and dynamic visual acuity*. In this aim, participants will be subjected to a tied-belt condition (belt-speed ratio of 1:1) as well as to a split-belt condition (belt-speed ratio of 1:3). For both conditions, participants will report the direction of Landolt-C optotypes projected at heel strike. The relative performance between these two conditions will be assessed in order to establish a relationship between locomotor asymmetry and the capacity for visual perception. I hypothesize that the perturbing effects of an imposed locomotor asymmetry will result in a less stable visual field. This reduction in visual field stability is expected to produce decrements in dynamic visual acuity.

Aim 2 *will examine the relationship between locomotor asymmetry and head stability.* Tri-axial accelerometers will be affixed to the forehead and tibiae of each participant in order to assess head-in-space equilibrium and shock attenuation. Head stability and shock attenuation will be assessed relative to belt-speed ratio (i.e., tied-belt vs split-belt) in order to establish a relationship between locomotor asymmetry and head stability. I hypothesize that the perturbing effects of an imposed locomotor asymmetry will hinder the capacity of the locomotor system to attenuate shock, thus causing a decrease in head stability.

Aim 3 *will examine the nature of visuomotor adaptation during imposed locomotor asymmetry.* As locomotor asymmetry (defined by step length asymmetry) approaches its baseline value during the 1:3 belt-speed ratio, it is expected that dynamic visual acuity will follow a similar trend. I hypothesize that this pattern of visuomotor adaptation will mirror that of locomotor adaptation due to the influence of the locomotor system on shock attenuation and head stability.

CHAPTER 2
REVIEW OF THE LITERATURE

2.1 Vision

2.1.1 Visual Information

Necessary to the understanding of visual perception is the understanding of visual information as it exists in the environment. In his seminal work *The Ecological Approach to Visual Perception* (Gibson, 1986), James Gibson proposes that the very notion of an environment is predicated on the existence of an organism within such environment. Though largely semantic, this distinction is worth addressing. The existence of an organism necessitates the existence of an environment – whether the environment is hospitable to the organism is wholly irrelevant. Conversely, by describing any geometric space as an *environment* it implies the existence of an organism within such space. Without the existence of the

organism – be it microbial or human – the environment forfeits its title as such and is relocated to the same category as all other geometric spaces. The fundamental existence of information, however, precedes the existence of both environment and species. Claude Shannon, in his development of Information Theory outlined the necessary components of a communication system. The components, as described by Shannon in *A Mathematical Theory of Communication* (Shannon, 1948) are as follows:

1) An *information source*, 2) A *transmitter,* 3) The *channel*, 4) The *receiver*, and 5) The *destination*.

In this context, an *information source* is the body that produces the message to ultimately be received by the *destination*. Consider, as Shannon did, the example of a telephone. In this case, the message is quite literally an auditory message – fluctuations in air pressure as a function of time. In order for this message to be received by the destination (e.g., a person on the other end of a phone call), it must first be converted into a transmissible form. This conversion is the role of the *transmitter*. Following the telephone example, the transmitter converts the air pressure function into a proportional function of electrical current. Once converted into electrical current, the signal is capable of being transmitted by the appropriate medium – a pair of twisted copper wires. This medium is described by Shannon as the *channel*. Before the message can be received at the destination, it must first be converted back into the original signal by the *receiver*. In effect, the receiver decodes the information that the transmitter previously encoded. Finally, the message has arrived at the destination – the "person (or thing) for whom the message is intended". This process, along with the introduction of noise into the signal, can be seen in *Figure 2.1* – taken from Shannon's 1948 publication.

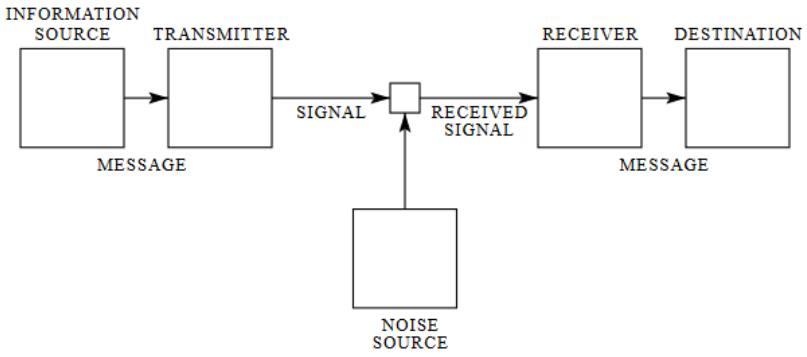

Figure 2.1 – "Schematic diagram of a general communication system" as described by Shannon.

The framework proposed by Shannon describes the system required for the intentional communication of a message between the information source and the destination through the use of communications technology. While this form of communication is no doubt of great importance, the form of communication with greatest relevance to this paper is of a more primitive nature – the receipt of visual information by an organism. To understand this form of communication and how it fits into Shannon's framework, consider the necessary components. The information source in this example is the physical space in which the organism (or destination, to follow Shannon's framework) exists. The existence of visual information within this space is not dependent upon the existence of the organism to perceive it, as Gibson suggests the space's status as an *environment* is. The existence of information, Shannon argues, is a fundamental property of a physical space – much the same as mass or volume. In the case of visual information, the physical space needs only to exist in order to produce a visually informative message.

Now consider the channel in Shannon's framework. In the case of the telephone, the transmitter only exists in order to transform the original message into a signal capable of being transmitted across the channel. In the telephone example, a pair of copper wires is incapable of transmitting fluctuations in air pressure, thus the necessity of a transmitter is apparent. In the case of an organism receiving visual information from its environment, however, the message need not be

converted into signal in order to arrive at the destination. Thus, the existence of the transmitter (and, by extension, the receiver) is unnecessary. Despite this system requiring no transmitter or receiver, the channel is not obviously identifiable. The message being conveyed, in the case of visual information, is light. The medium through which light travels is entirely dissimilar from that through which a telephone signal travels; light is capable of traveling infinitely, without decay, through media and vacuum alike (Heeck, 2013). Indeed, conceptualizing the requisite channel for a visual message to be propagated through is so difficult that it has plagued the minds of both De Broglie and Einstein. In 1920, following the birth of the general theory of relativity, Albert Einstein pondered the existence of such a medium (Einstein, 1920): *"We may say that according to the general theory of relativity space is endowed with physical qualities; in this sense, therefore, there exists an Aether. According to the general theory of relativity space without Aether is unthinkable; for in such space there not only would be no propagation of light, but also no possibility of existence for standards of space and time (measuring-rods and clocks), nor therefore any space-time intervals in the physical sense. But this Aether may not be thought of as endowed with the quality characteristic of ponderable media, as consisting of parts which may be tracked through time. The idea of motion may not be applied to it."* Suffice to say that the channel through which visual information must travel – be it air, vacuum, or ether, exists in abundance in the environment of question. The destination, then, is the final component of the system required for the receipt of visual information by an organism. In the case of a human, Shannon's framework is complete the moment light reaches the eye. At the end of Shannon's framework, however, lies an expanse of other frameworks – all dealing with how it is that the destination is able to *perceive* such information.

Perhaps the most obvious difference between the example of a telephone conversation between two people and a visual message between an organism and its environment is the direction of information travel. In the case of two people communicating via telephone, information is exchanged in both directions. This differs from the example of an organism and its environment where

information is not actively exchanged but received by one party and disseminated by the other. Another obvious difference, following this example, is that of intent. In order for a telephone conversation to be successful, both parties must have the intent to exchange information. This differs again from the example of an organism and its environment in that the environment will disseminate visual information by virtue of its existence, thus shifting the full burden of intent onto the organism if the message is to ever be received. This intent is underscored in Gibson's suggestion that *natural vision* is exploratory in nature (Gibson, 1986); consisting not only of the eyes, but of the organism's inclination to "look around, walk up to something interesting and move around it so as to see it from all sides, and go from one vista to another". In this case, the exchange is not of information for information, but of information for action. When the organism moves relative to its environment, for example, the dynamic pattern of visual information resulting from the organism's movement (known as optic flow) informs the organism on how subsequent movements might be optimized. Acting upon this information, the organism may choose to modulate any subsequent forces it applies on the environment, thus further influencing the available information (W. H. Warren, 1990). This cycle, known as *perception-action coupling*, is the basis for the *ecological approach* to perception – the lens through which this paper will attempt to answer all pertinent questions related to sensory perception and the control of action. *Figure 2.2* illustrates the *perception-action cycle* as it relates to an organism navigating through its environment – taken from Warren (1990).

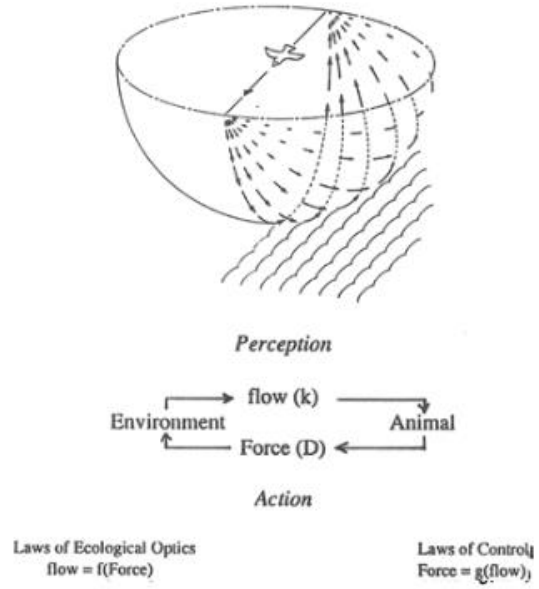

Figure 2.2 – The perception-action cycle, in which the perception of optic flow influences the forces applied by the animal on the environment, which further influences the state of the optic flow.

2.1.2 Visual Pathways

Though the eyes are most closely associated with the sense of sight, it would be wrong to attribute the entirety of the visual experience to the eyes alone. Indeed, the reception and subsequent rudimentary processing of visual information by the eyes does not give rise to the human visual experience. Such a level of visual perception requires the processing and integration made possible only by dedicated visual centers of immense complexity, such as those found in the brain. The visual experience, then, is the product of an intricate system of communication between the environment and relevant sensory subsystems. Thus, if one is to understand the visual system in its entirety, one must be familiarized with the anatomical pathways through with visual information travels and is subsequently processed. In this section, the relevant anatomical structures and pathways will be reviewed.

The only region of the vertebrate eye capable of processing visual information is known as the *retina*. The deepest layer of the retina, located farthest from external sources of light, is comprised entirely of *photoreceptor cells*. It is the job of these cells to convert light into a neural signal capable of

being transmitted along the visual path (to follow Shannon's telephone example, these cells may be thought of as transmitters – converting light into a signal form capable of being transmitted via synaptic connections). Once the light is converted into the appropriate neural signal, it is transmitted first to the bipolar cells, then to the amacrine and retinal ganglion cells. The axons of the retinal ganglion cells converge to form the *optic nerve*, through which the neural signal exits the eyes and travels towards the brain (Kandel, E.; Schwartz, J.; Jessel, 1991). It is worth noting that while the above process introduces the general pathway for visual information in humans, not all neural connections exist in such a linear fashion (such as in the case of synaptic connections between adjacent photoreceptors, or between photoreceptors and horizontal cells). In *Figure 2.3*, the five major cell types of the retina can be seen – taken from Tresilian (2014).

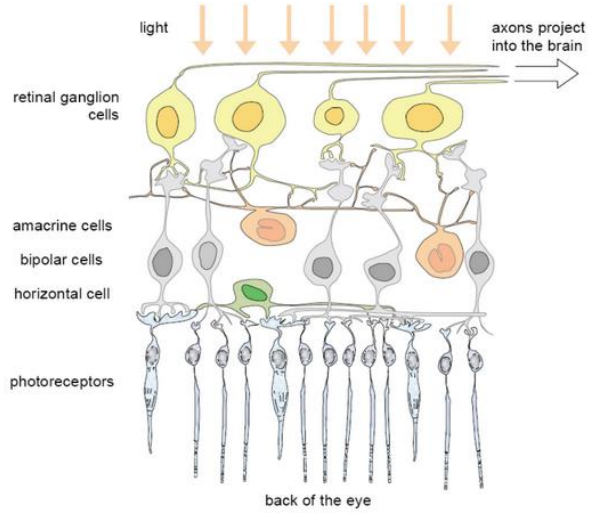

Figure 2.3 – The five major cell types comprising the retina – retinal ganglion cells, amacrine cells, bipolar cells, horizontal cells, and photoreceptors.

Before any light can reach the retina, however, it must first pass through the *pupil* and the *lens*. The pupil functions to regulate the amount of light that is let into the eye (and, by extension, onto the retina) while the lens functions to *focus* entering light onto the retina as to produce a clearer image. The lens is able to focus light onto a particular point on the retina by virtue of its shape as a convex lens. Convex lenses (known also as convergent lenses) function to refract any light which passes

through onto or towards a single point known as the principal focus. The location of the principal focus is typically dependent upon 1) the focal distance and 2) the optical power of the lens. In the case of the human eye, however, the principal focus is restricted to a specific point on the retina known as the *fovea*. The fovea, while comprising only three to four percent of the retinal area, is the point of highest visual acuity in the human eye. This is due primarily to the density of *cones* (photoreceptors specialized for visual acuity) found within the fovea, though other structural features are responsible as well. For example, the cells that light must normally pass through in order to reach the photoreceptors are pushed aside in the center of the fovea, creating a clear path for light to travel without being scattered or absorbed. In order to maintain the principal focus directly on the center of the fovea (which is at a constant focal distance), the lens must alter its optical power through a process known as *accommodation*. During accommodation, the musculature surrounding the lens, known as the *ciliary muscle*, contracts and relaxes in order to change the curvature (and thus the refractive power) of the lens. When an object is close to the eye, for example, the ciliary muscle will contract in order to increase the curvature and refractive power of the lens. Conversely, when an object is farther away, the ciliary muscle relaxes in an effort to decrease the curvature and refractive power of the lens (Tresilian, 2012).

Such elaborate mechanisms exist to aid in the reception and encoding of information from the visual field. As mentioned previously, however, the reception of such information by the eyes does not directly result in the visual experience we are familiar with. Rather, it is the processing and integration of such information that gives rise to visual perception. While a majority of this processing and integration occurs in the visual cortex, the processing capabilities of the retina should not be discounted. Note that in *Figure 2.3* the number of photoreceptors far exceeds the number of retinal ganglion cells, suggesting that several photoreceptors must converge onto a single retinal ganglion cell. The area on the retina occupied by a network of photoreceptors that converge onto a given retinal

ganglion cell is known as that ganglion cell's *receptive field*. Visual processing begins here and is heavily influenced by the configuration of individual receptive fields. A majority of retinal ganglion cells, for example, exhibit what is known as *spatial opponency* – a phenomenon where the stimulation of photoreceptors in one region of the receptive field will result in the ganglion cell's excitation, while the stimulation of photoreceptors in another region will result in its inhibition. Such configurations result in the first level of visual processing, where spatial and temporal patterns of stimulation are encoded in the neural signal that exits the eyes via the optic nerve (Kandel, E.; Schwartz, J.; Jessel, 1991). An idealized example of spatial opponency can be seen in *Figure 2.4* – taken from Kandel (1991).

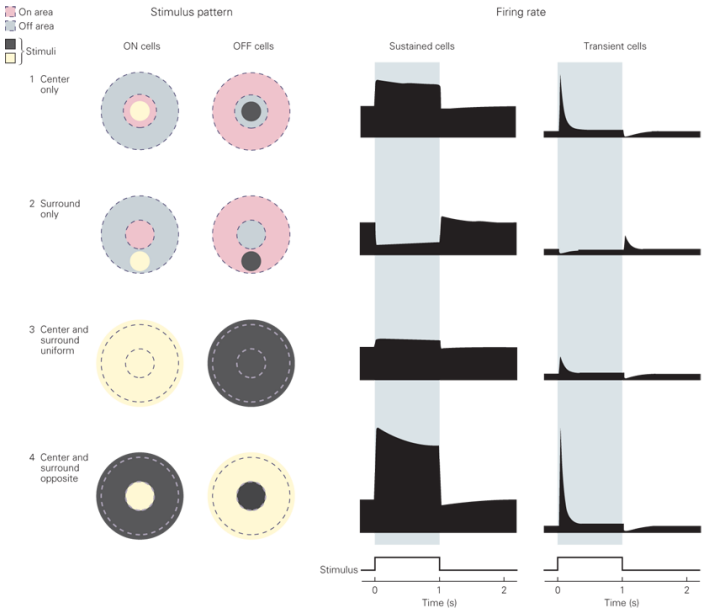

Figure 2.4 – Retinal ganglion cells exhibiting a type of spatial opponency known as center-surround opponency. In this case, differential stimulation of photoreceptors in the center versus the surround of the receptive field will result in excitation of the retinal ganglion cell. Note that uniform stimulation of photoreceptors in both the center and the surround of the receptive field, as seen in example three, evokes a relatively weak response (see electronic copy for colored version).

As the neural signal travels along the axons of retinal ganglion cells, several pathways emerge. The largest pathway, known as the *geniculostriate pathway,* travels from the retinas to the *primary visual cortex (V1)*. The neural signal is carried first by the axons of retinal ganglion cells to the *lateral geniculate nuclei*, then from the axons of the lateral geniculate nuclei (known as the *optic radiations*) to

the primary visual cortex. The primary visual cortex is considered to be responsible for conscious visual perception, as damage to this area results in the loss of visual awareness. It is worth noting that the spatial organization of the receptive fields is conserved along the geniculostriate pathway, such that the topographic pattern of the retina is reflected on the primary visual cortex. Given that the relative density of photoreceptors (and, by extension, the relative density of receptive fields) is greatest in the foveal region of the retina, the region of the primary visual cortex that is analogous to the fovea is considerably larger than other regions. Eventually, the neural signal is transmitted along the visual cortex towards areas of further specialization, where complex networks of neurons continue to process and integrate the encoded information. The identification of such areas, however, is beyond the scope of this paper (Kandel, E.; Schwartz, J.; Jessel, 1991; Tresilian, 2012).

While the structures and pathways described in the above paragraphs are essential for understanding the visual system, such description alone is insufficient to explain the nature of visual perception in humans. In the following sections, visual perception will be explored as a complex system capable of extracting spatial and temporal information from the visual field.

2.1.3 Visual Perception

A number of theories and hypotheses have been developed with the goal of discerning what information from the optic flow is used by animals to navigate within their environments. Perhaps the most well-known is David Lee's *Tau Theory*, in which the relative rate of expansion for a given retinal image is used to perceive the time it will take for the animal to make contact with the object in question (D. N. Lee, 1976). *Figure 2.5* provides a simplified illustration of this concept (Tresilian, 2012). In Panel A, the distance from the human's eye to the start of the gap is labeled D, and the width of the gap is labeled W. Panel B provides an illustration of how light rays reflected off of the edges of the gap will cross the lens and project onto the flattened retina. Note that in this panel the distance between

the lens and the flattened retina is labeled *f*, and the distance on the flattened retina corresponding to the width of the gap is labeled *w*. At this point, it is apparent that as the human approaches the gap (distance D decreases) the image width (distance *w*) will increase. This can be expressed mathematically as follows: D x *w* = *f* x W. Given the invariance of *f* and W, one can deduce that the rate of change of *f* and W are inversely proportional. For this reason, the rate of change of D (expressed as V) must be proportional to the rate of change of *w* (expressed as ε). Thus, D/V is equal to *w*/ε.

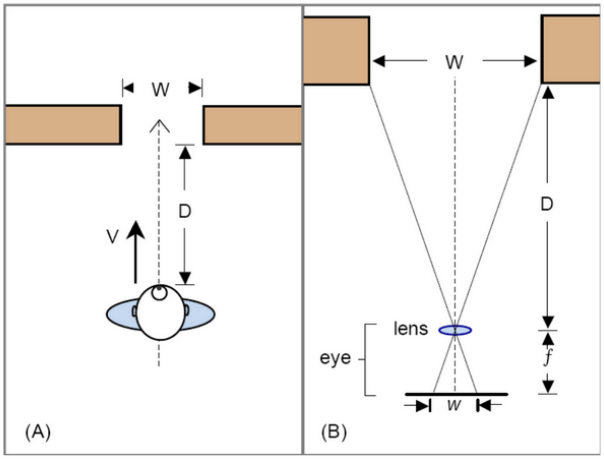

Figure 2.5 – A simplified schematic of the spatial components necessary for an animal to perceive the time it will take to make contact with an object or point in space - Figure taken from Tresilian (2014)

This equation, D/V = *w*/ε, is at the heart of Tau Theory, providing an elegant (albeit simplified) mathematical description of how time-to-contact might be perceived in dynamic conditions. Following *Figure 2.5*, one can see that the left hand of the Tau equation (D/V) is equal to the time it will take for the human to make contact with (or arrive at) the gap. Given that the right hand of the equation (*w*/ε) uses only the retinal image width (*w*) and the rate of the retinal image width's expansion (ε), it becomes clear that all necessary information required to perceive the time it will take to make contact with an object in the environment is readily available (D. N. Lee, 1976).

It is important to note that while the above Tau equation provides useful information regarding time-to-contact, it is limited to conditions where the animal is traveling at constant velocity. If, for

example, the human in *Figure 2.5* were to increase speed while approaching the gap, the provided Tau equation would be insufficient. It is worth mention, however, that this error between the predicted and actual TTC is inversely related to the speed of travel. For example, a diving gannet approaching the water's surface at 1 m/s would incur an error of 100% the time-to-contact, while the error incurred by a gannet approaching the water's surface at 10 m/s would amount to only 15% the time-to-contact (David N. Lee & Reddish, 1981). Nonetheless, the presence of a calculable error in this simplified mathematical model often begets the question of why *time* and not *distance* is the perceived variable of interest. The answer to this question is two-fold: one theoretical component concerning the process of dynamically perceiving distance, and another experimental component concerning commonalities in animal behavior. Regarding the theoretical basis for distance being the variable of interest, one can assume that explicit distances cannot be computed simply by perceiving a static visual field. For this reason, it would be necessary to obtain both timing and velocity information as to calculate an explicit distance measure. While this is certainly possible, it is unlikely that movement is reliant upon both an error-prone internal clock and a velocity perception mechanism that is as complicated as the entirety of Tau Theory. Concerning the experimental results, Lee demonstrated in 1981 that diving gannets prepared for plunging underwater at similar times (approximately 820 milliseconds) by tucking their wings into a streamline shape (David N. Lee et al., 1981). Why then, if distance was used as opposed to time, would this preparatory behavior be demonstrated at similar times across animals but not similar distances?

Similarly, two competing hypotheses have attempted to describe what information from the optic flow is used to navigate or steer towards a goal in three-dimensional space. The first, referred to in this section as the *Direction Hypothesis*, suggests that navigation towards a target is done by simply aligning the body in the direction of the target and locomoting straight towards it (Rushton, Harris, Lloyd, & Wann, 1998). The second, referred to here as the *flow hypothesis* suggests that the direction

of locomotion is aligned with the *focus of optic expansion* rather than the target itself (Gibson, 1950). Normally, the focus of optic expansion would emerge directly from the target during locomotion, making it impossible to dissociate the two sources of information (see *Figure 2.6*).

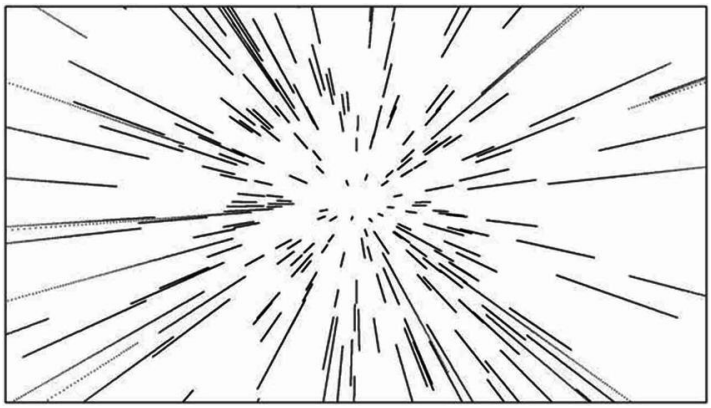

Figure 2.6 – An illustration in which the focus of optic expansion is located at the center of the image.

In an effort to disentangle the two, Warren and colleagues devised an experiment in which virtual reality would be used to violate the laws of optics such that the focus of optic expansion and the target direction were no longer the same (J. Warren, Kay, Zosh, Duchon, & Sahuc, 2001). This was done by placing a head-mounted virtual reality display on the participants while they were allowed to walk freely within the laboratory. Head position feedback was collected and integrated into the system at 60 Hz, allowing for updates to the virtual environment. The angle between the actual heading direction and the focus of optic expansion (0 degrees in normal conditions) was offset by 10 degrees so that if the participants were to walk with the focus of optic expansion placed on the target, they would in fact be walking slightly to the left or right of the target. Likewise, if the participants were to steer by aligning the target with their egocentric directions, the focus of optic expansion offset would yield a virtual heading error of 10 degrees. This process allowed Warren et al. to discern which hypothesis was closer to the actual path taken by the participants.

To account for any effect that information density in the virtual environment might have on navigation strategy, four conditions were created. Condition A offered the least amount of visual

information, with the target being a thin red line with no visible floor, ceilings, walls, or texture. Condition B displayed the same thin red line as the target, this time with the inclusion of a textured floor. Condition C offered a doorway as the target in an environment complete with a floor, ceiling, and walls. Condition D offered the same environment as in Condition C, this time with the addition of columns throughout the environment.

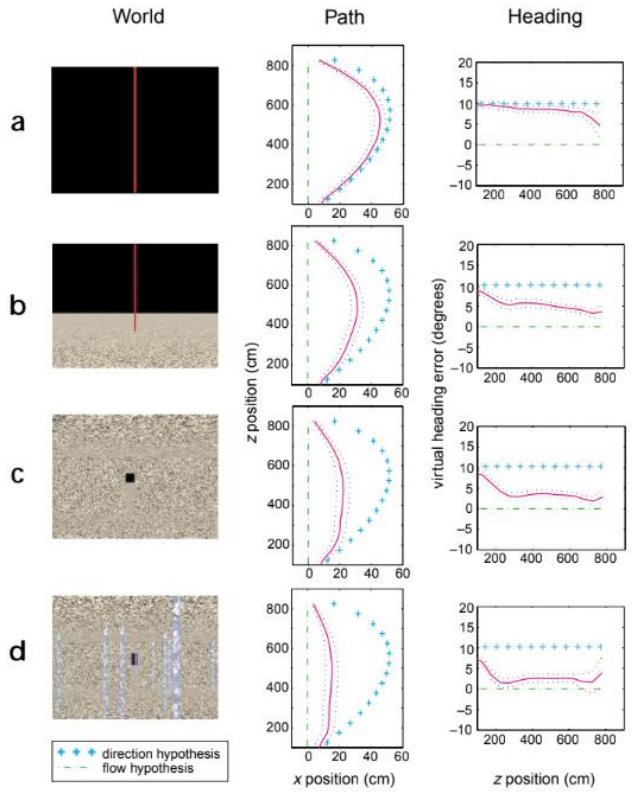

Figure 2.7 - The four virtual reality conditions, along with 1) the average of the experimentally recorded paths for each condition, 2) the path predicted by the direction hypothesis, and 3) the path predicted by the flow hypothesis (see electronic copy for colored version).

Following the work of Warren et al.(J. Warren et al., 2001), neither the proponents of the flow hypothesis nor of the direction hypothesis could lay claim to absolute victory. *Figure 2.7*, in addition to offering a sample image of each virtual environment, displays the paths taken by the participants plotted against the paths predicted by both the direction and flow hypotheses for each of the four environmental conditions. What Warren et al. found was that the relative use of egocentric direction and focus of optic expansion to locomote towards a target is entirely dependent upon the density of

available visual information in the environment. Looking at *Figure 2.7*, one can see that the paths taken by the participants rely more heavily upon the focus of optic expansion as the environment becomes saturated with more and more visual information. For example, condition A provides no more visual information than a thin red line as the target, thus participants relied almost entirely on egocentric direction. As visual information was added, however, the participants' paths moved closer and closer towards the path predicted by the flow hypothesis, suggesting that the focus of optic expansion is increasingly relied upon as visual information is added to the environment. Ultimately, Warren et al. were able to demonstrate that while the focus of optic expansion and egocentric direction during locomotion are typically redundant in natural environments, the visual system tends to rely more heavily on one of these two strategies depending on the available information. As a result, locomoting towards a goal in an environment lacking in visual information (an open field) might rely more heavily on egocentric direction, whereas locomoting towards a goal in an environment rich with visual information (a dense forest) might rely more heavily on the focus of optic expansion.

The work of Warren and Lee have no doubt contributed to the field of visual perception by establishing how it is that visual information might be perceived. In the following sections, the mechanisms employed by the body to establish and maintain the necessary conditions for optimal visual perception will be explored.

2.2 Locomotion

2.2.1 Self-Optimization

The evolutionary drive for complex, adaptable movement is responsible for much of the morphological variation seen across species. When this movement is implemented in such a way that it permits an organism to navigate within its environment, it can be described as *locomotion*. Essentially,

locomotion is the product of successive reactionary forces from the environment on an organism. It is for this reason that the morphologies of all species within the animal kingdom are ideally suited to apply forces to their natural environments – a bird, for example, has evolved wings and a fanned tail to optimize aerodynamic forces; a squid has evolved a mantle to optimize jet-propulsive forces; and a human has evolved legs to optimize ground reaction forces (Dickinson et al., 2000). It is tempting, then, to think that the study of locomotion consists only of examining the movement of an animal during locomotion through the lens of classical mechanics. Reducing the entirety of locomotion to its mechanical basis, however, is akin to reducing the entirety of visual perception to the function of the photoreceptors. For this reason, the following sections will examine human locomotion across multiple levels of study as to provide a more comprehensive review.

Having evolved to be both mechanically stable and energetically efficient, human locomotion exploits the oscillatory nature of center-of-mass movement. In walking, for example, the sinusoidal pattern of the center-of-mass can be modeled as an inverted pendulum in which kinetic and gravitational potential energy are inversely coupled (Kuo, Donelan, & Ruina, 2005). This coupling is a result of the passive dynamics of bipedal locomotion, in which the center of mass is vaulted over the stance leg, attaining its highest position at midstance before returning to its lowest position during the step-to-step transition (see *Figure 2.8*). As the center of mass travels towards its highest position, its kinetic energy is converted to gravitational potential energy (Kuo, 2007). As is the case with pendulums, though, the cyclical energy in the system will dissipate through conversion to heat and sound. For this reason, both humans and pendulums require a force-actuator if motion is to continue. In the case of human walking, the skeletal muscles of the lower extremities act as force-actuators, applying propulsive torques at the step-to-step transition where gravitational potential energy is at its lowest. Unlike conventional pendular systems, however, the human locomotor system operates under evolved metabolic constraints in which the application of the requisite energy is optimized by the system

(Hamill et al., 1995). Perhaps the most elegant example of this optimization is the self-selection of a stride frequency that correlates with 1) the resonant frequency of the system when modeled as a force-driven harmonic oscillator and 2) the minimum metabolic work required to sustain constant-speed locomotion (Holt, Hamill, & Andres, 1991). Such correlations underscore both the self-optimizing capacity of the locomotor system as well as the relative accuracy of the inverted pendulum model.

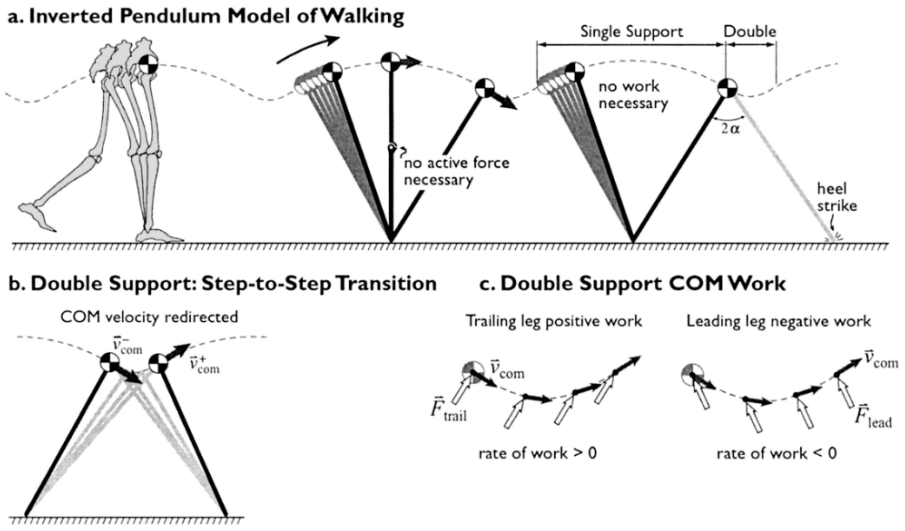

Figure 2.8 – An illustration depicting the inverted pendulum model of human locomotion, in which the lower extremity is a rigid, massless support rod and the mass of the body exists as a single point sitting atop the lower extremity – Figure taken from Kao et al. (2005)

While mechanical models of walking may prove useful in the estimation of kinematic, kinetic, and energetic variables, such models do little to address the adaptable nature of human locomotion. In the following sections, the neural drive responsible for the generation and adaptation of locomotor parameters will be discussed.

2.2.2 Neural Control

The human body, with its hundreds of muscles and joints, is a multiplicity of freedom and flexibility. Assembling the redundant degrees of freedom inherent to such a body is a complex task that requires organizing the constituent units in a fashion that is both goal and context dependent (Turvey,

1990). In the case of the human body during locomotion, the exact mechanism of such organization is not well understood. In this section, a framework aimed at elucidating the requisite levels of neural control for stable, adaptable bipedal locomotion will be introduced. Such a framework, in order to describe the necessary levels of control, must consider both volitional and involuntary control mechanisms, as well as the influence of environmental information on the system in its entirety.

Attempts to distinguish involuntary or reflexive actions from those guided by conscious effort appear in philosophical literature dating back to the 17th century, such as in Rene Descartes' attempt to identify the metaphysical origins of action. In his seminal work "Passions of the Soul," Descartes attempts to disentangle the volitional from the involuntary, attributing the former to the soul and the latter to the inescapable reach of animal spirits to which we are bound (Descartes et al., 2012): "*If someone suddenly thrusts his hand in front of our eyes as if to strike us, then even if we know that he is our friend, that he is doing this only in fun, and that he will take care not to harm us, we still find it difficult to prevent ourselves from closing our eyes. This shows that it is not through the mediation of our soul that they close, since this action is contrary to our volition, which is the soul's only activity, or at least its main one. They close rather because the mechanism of our body is so composed that the movement of the hand towards our eyes produces another movement in our brain, which directs the animal spirits into the muscles that make our* eyelids *drop."* Descartes, while unable to precisely identify the origin of action, was correct in his assertion that volitional action has a dissimilar origin from that of involuntary action. Indeed, the origins of volitional and involuntary actions differ not only in their neural pathways, but in their respective origins more fundamentally. Volitional movement, while often influenced by external, environmental information, is ultimately a product of signals produced in the body itself. That is to say, the soul which Descartes describes is the very notion of voluntary control as it exists in the mind and body. Dissimilarly, involuntary movement, while often subject to the influence of volitional control, is ultimately a product of environmental information. In

this sense, the signal required to produce an action might originate from internal or external sources in the case of volitional and involuntary actions, respectively.

In order for complex, functional movements such as locomotion to be both adaptable and goal directed, volitional and involuntary influence must be coordinated across all levels of complexity. Take, for example the *autogenic stretch reflex*, in which a skeletal muscle contracts in direct response to strain. While the autogenic stretch reflex is remarkably simple in nature, it is important to note that this reflex is *not* what could be considered an *elemental reflex* due to the fact that it can be meaningfully broken down into further individual components (Matthews, 1991). These sub-components, associated with various levels of volitional control, can be seen below in *Figure 2.9*.

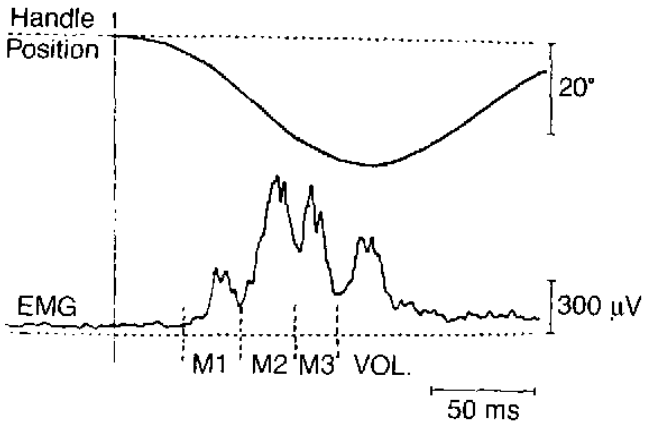

Figure 2.9 - Electromyographic response of wrist extensors to forceful wrist flexion. Wrist flexion was applied by changing the position of a handle that participants were instructed to grasp and keep steady. EMG response can be meaningfully segmented in four sub-components: M1, M2, M3, and VOL – Figure taken from Matthews (1991).

Note that in the above figure, each of the four EMG peaks occur at different times following the perturbation, suggesting that multiple neural pathways of various lengths may be involved. The EMG peak labeled M1, for example, typically occurs with a delay consistent with that of a monosynaptic spinal reflex (25 to 50 milliseconds following perturbation) (Liddell & Sherrington, 1924). M1, then, is considered to be a true spinal reflex, both due to the stereotyped time delay, as well as from an

abundance of literature in which spinalized animals continue to exhibit the M1 response (Chapter 16 Functional plasticity following spinal cord lesions, 2006). Peaks M2 and M3, in contrast, have latency periods longer than that of M1, typically occurring 50 to 100 milliseconds following induced strain (Forgaard, Franks, Maslovat, & Chua, 2016). This increased delay, in conjunction with the absence of the M2 and M3 responses in spinalized animals, suggests that these responses are supraspinal (Frigon, Johnson, & Heckman, 2011). Finally, the VOL peak is associated with the voluntary contraction of the perturbed muscle. This association is made as a result of both the latency period of the response (typically between 150 and 200 milliseconds), and because this peak is absent when participants are instructed *not* to resist the perturbation (Tresilian, 2012). It is worth mentioning that when participants are instructed not to resist the perturbation, peaks M2 and M3 greatly decrease in amplitude, suggesting a degree of volitional inhibition exists over these pathways (Tresilian, 2012). If muscles responded to perturbations in a purely reflexive, stereotyped fashion without the capacity for modulation, complex tasks such as bipedal locomotion would forfeit their unique combination of adaptability and goal-directedness. While such modulation is essential for the *regulation* of such tasks, it is not sufficient to explain how such tasks are generated or sustained.

Central to this concept, then, is the existence of neuronal circuits that are capable of intrinsically generating the rhythmic movements necessary for both walking and running. These circuits, referred to as *central pattern generators* (CPGs), are thought to produce the requisite oscillatory movement patterns necessary for bipedal locomotion in the absence of both cortical control and sensory feedback. Note that while the existence of CPGs has been confirmed experimentally in reduced animal models, evidence of their existence in humans is limited (Dimitrijevic, Gerasimenko, & Pinter, 1998; McLean, Masino, Koh, Lindquist, & Fetcho, 2008). Still, the existence of CPGs in humans is plausible both phylogenetically and functionally, leading researchers to develop a multitude of CPG models aimed at sufficiently describing the architecture and functional limitations of such neural circuits. By

providing accurate models describing how central pattern generators might contribute to the production of bipedal locomotion, researchers will be better equipped in their endeavor to develop effective neurorehabilitation strategies for those with neurological impairment.

Various CPG models have been proposed over time with the goal of summarizing how rhythmic movement patterns might emerge from a neural network. Central to any CPG model are two main components; the first of which is a method of taking a tonic signal that is put into the network and using it to produce a rhythmic output; the second of which is a method of creating inhibitory coupling at the functional level that produces anti-phase contraction patterns in antagonistic muscle groups (e.g., leg flexors and extensors during walking). Despite the aforementioned commonalities between all CPG models, the origin of rhythmic patterns is not yet fully understood nor agreed upon. Eve Marder addresses this concern by outlining two possible mechanisms underlying the production of rhythmic patterns (Marder & Bucher, 2001). *Figure 2.10* (below) offers a graphical representation of the two main mechanisms capable of producing a rhythmic output resulting from a tonic input. While the outcome is the same in both conditions, the underlying mechanisms are not. The top panel in *Figure 2.10* displays coupling between a pacemaker neuron and a neuron with no intrinsic rhythmic characteristics. In this case, a "follower" neuron is paired with the pacemaker cell, thus causing the network to adopt and magnify the rhythmic characteristics of the pacemaker. Pacemaker-driven networks have been found to produce functional movements in crustaceans, implying that a similar mechanism may have been conserved in humans (Hooper & Marder, 1987). In contrast, the bottom panel in *Figure 2.10* depicts inhibitory coupling between two neurons – neither of which have intrinsic rhythmic properties. The rhythmic signal that emerges from this example is a result of inter-neuron dynamics, where fatigue in one neuron may cause the system to fall into an anti-phase pattern. Ultimately, both mechanisms provide a reasonable explanation for how it is that oscillatory neuronal activity might emerge and subsequently generate rhythmic movement at the functional level.

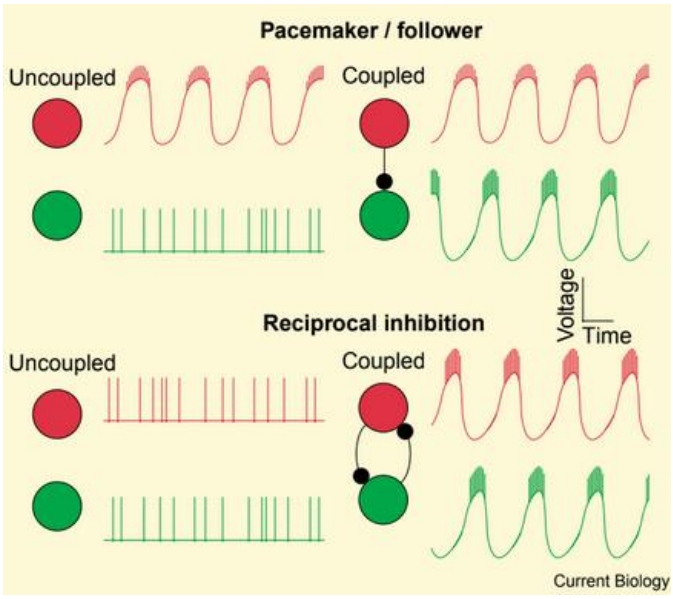

Figure 2.10 – Two possible origins of rhythmic signal production at the neuronal level – Figure taken from Marder et al. (2001).

In order for humans to execute complex tasks such as bipedal locomotion, neural input across all levels of the volitional hierarchy must contribute *in parallel* to the initiation, generation, and sustainment of movement. The decision to locomote, for example, results from volitional control within cortical region. Likewise, the reflexive capacity of the human system to make appropriate, rapid adjustments based on environmental information is primarily the result of complex spinal networks. Finally, the repetitive, oscillatory nature of bipedal locomotion, while *initiated* by supra-spinal centers, must be sustained involuntarily by neural circuits residing peripherally. Together, the volitional hierarchy is a complex system capable of responding to ecological perturbations in a non-stereotyped, yet highly reflexive fashion.

2.2.3 Locomotor Asymmetry

Human walking, when not perturbed by ecological factors or neuromechanical impairment, is relatively symmetrical with spatial and temporal parameters being roughly mirrored between limbs (D. S. Reisman, Block, & Bastian, 2005). Such symmetry is thought to contribute to the energetic

optimization of locomotion, as asymmetrical gait is often associated with an increase in metabolic cost (Finley & Bastian, 2017). When the human locomotor system is perturbed, however, certain parameters of symmetrical gait are typically restored after continued exposure to the perturbation, underscoring both the adaptable nature of the system and the natural bias of the system towards symmetry (Finley, Bastian, & Gottschall, 2013). Exploring the adaptive capacity of the locomotor system in healthy humans, then, requires exposure to an environment in which a perturbation can be both readily controlled and measured.

In 1993, Volker Dietz and colleagues first exposed healthy adult human subjects to a treadmill with two independent belts, such that the speed of each limb could be controlled independently (Dietz et al., 1994). Exposure to this treadmill was found to elicit profound biomechanical and electrophysiological changes, suggesting that neuronal networks at the spinal level might be responsible for independent control of the limbs. Likewise, while changes to stance and swing phase durations necessarily persisted throughout exposure to the perturbation, participants were found to adapt to the condition over the course of 15 to 20 step cycles (Dietz et al., 1994). Like all motor adaptation experiments, exposure to the split-belt treadmill produced both an adaptation and an after-effect, following exposure to and removal of the perturbation, respectively. In fact, the presence of such an after-effect is widely considered to be the defining feature of any adaptation (Roemmich et al., 2018). To date, the split-belt adaptation paradigm has been expanded to assess the effects of age (Vasudevan, Torres-Oviedo, Morton, Yang, & Bastian, 2011), visual information (Torres-Oviedo & Bastian, 2010), neurological deficits (Morton & Bastian, 2006), and attentional constraints (Malone & Bastian, 2010) on locomotor adaptation in humans.

In its most basic form, the split-belt paradigm consists of exposing the participant first to the treadmill in its tied-belt state, where both belts move at identical speeds as they would on a conventional treadmill. Typically, this baseline period will consist of two minutes at the speed of the

slow belt, followed two minutes at the speed of the fast belt in order to assess gait parameters during symmetrical locomotion at both speeds. In the adaptation period, a limb will typically be assigned randomly to the fast-belt, and the participant will be instructed to walk for approximately ten minutes with one limb moving two or three times faster than the other (Torres-Oviedo, Vasudevan, Malone, & Bastian, 2011).

Upon exposure to the split-belt condition, two distinct categories of adaptation are typically observed over different timescales (D. S. Reisman et al., 2005). Immediately following the split-belt perturbation, for example, changes to kinematic parameters such as duration of stance and swing occur in order to accommodate the change in belt speeds, as the limb on the slow belt must increase its duration in stance if the body is to maintain position on the treadmill. Note that this reactive change in the duration of stance and swing is mirrored when the treadmill is returned to the post-adaptation tied condition (D. S. Reisman et al., 2005). Dissimilarly, gait parameters most closely associated with inter-limb coordination such as step length and step time asymmetry tend to adapt *predictively* (i.e., in stereotypical fashion over the course of many strides) as exposure to the perturbation persists (D. S. Reisman et al., 2005).

The post-adaptation period typically occurs immediately following the adaptation period and consists of returning the treadmill to a tied-belt condition where both belts travel at the speed of the slower belt for approximately five minutes. During this post-adaptation period, the presence of after-effects (that is, the opposite asymmetry as observed during exposure to the split-belt perturbation) suggests that motor adaptation has occurred (Roemmich et al., 2018). A schematic depicting the split-belt adaptation paradigm can be seen below in *Figure 2.11*.

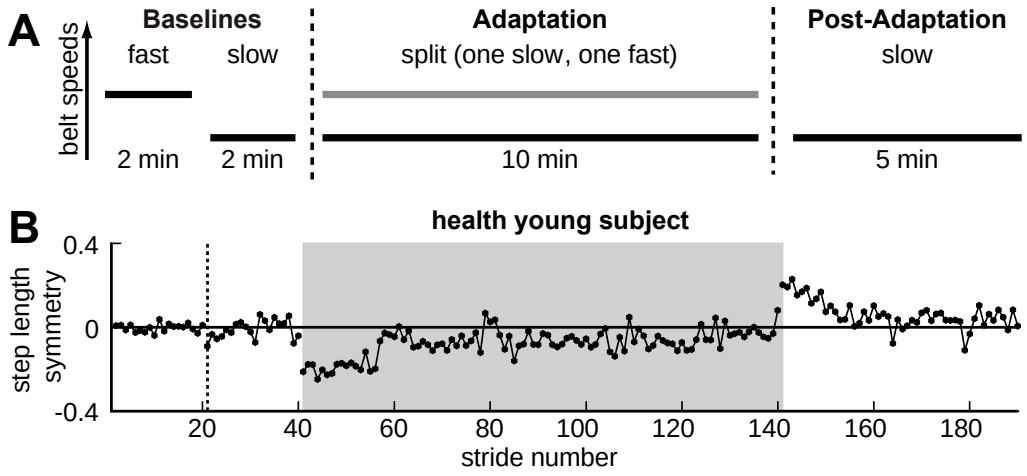

Figure 2.11 – (A) Split-belt treadmill paradigm displaying treadmill belt speeds for 1) the tied-belt baseline, 2) the split-belt adaptation period, and 3) the tied-belt post-adaptation period. (B) Step length symmetry for a healthy adult measured across the paradigm (note that step length symmetry of 0 indicates perfect symmetry). Figure taken from "NSF Grant 2018 – Choi, Van Emmerik, & Hamill"

The after-effects seen during the post-adaptation period have been the target of several neurorehabilitation interventions, particularly for those with hemiparesis (Malone et al., 2010; Torres-Oviedo et al., 2010). In the case of persons with cerebral damage stemming from stroke or hemispherectomy, locomotor asymmetry is typically observed (D. Reisman et al., 2013). When participants with hemiparesis are exposed to the split-belt paradigm, the perturbation typically serves to increase the magnitude of the asymmetry during the adaptation period (Roemmich et al., 2018). Importantly, participants with hemiparesis will undergo the same motor learning adaptation that healthy participants do, approaching baseline symmetry after approximately ten minutes (Roemmich et al., 2018). Note that while baseline symmetry in healthy participants means symmetrical step lengths, baseline symmetry in hemiparetic participants is *not* symmetrical; it is simply the baseline level of asymmetry that would be observed during over-ground or tied-belt walking. During the post-adaptation period, then, the opposite asymmetry occurs when the belts are returned to the tied-belt state. While for healthy participants this reversed asymmetry means there will be an equal but opposite asymmetry to their initial exposure to the split belt condition, the reversal of the initial

asymmetry for those with hemiparesis means that gait parameters will be relatively symmetrical when compared with baseline (Roemmich et al., 2018). These after-effects – which ultimately serve to reduce the asymmetry in overground walking for persons with hemiparesis – have been documented to last from just a few minutes (D. S. Reisman, Wityk, Silver, & Bastian, 2007) to several months (D. Reisman et al., 2013), depending on the magnitude and frequency of the training stimulus.

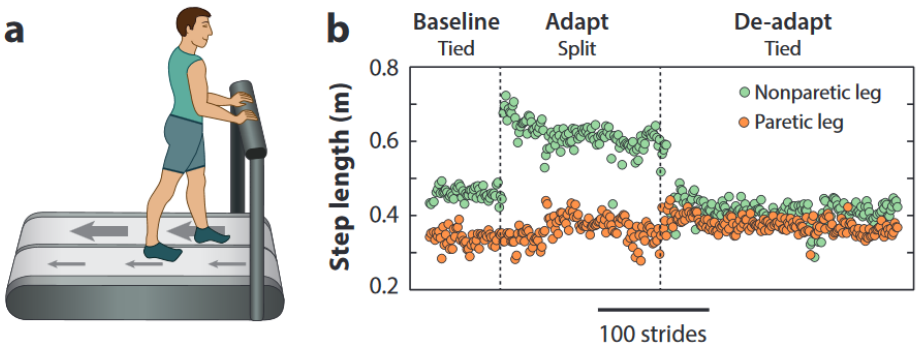

Figure 2.12 - (A) Depiction of a person walking on a split-belt treadmill. (B) Step length data during the split-belt treadmill paradigm from a participant with hemiparesis. Note that the step lengths are nearly equal during the de-adaptation period when compared with baseline - Figure taken from Roemmich & Bastian (2018).

The storage of motor learning such that after-effects translate to different environments is known as *transfer*, and has been the focus of many studies working with the split-belt paradigm (Torres-Oviedo et al., 2010). Perhaps the most relevant of these studies to this review comes from Gelsy Torres-Oviedo and Amy Bastian, in which transfer was examined as a function of visual information (Torres-Oviedo et al., 2010). By removing vision during the split-belt adaptation, participants were found to increase transfer to overground walking, thus implying that disrupting environmental cues might expand the training stimulus. Whether the increased transfer observed in this study was due to an alteration to the internal model, as suggested by Torres-Oviedo and Bastian, is beyond the scope of this review (Torres-Oviedo et al., 2010). However, the results do suggest that

multisensory integration plays a valuable role in the storage of motor learning adaptations. For this reason, the interaction of the locomotor and visuomotor systems ought to be further explored.

2.3 Dynamic Vision

2.3.1 Multisensory Integration

Performing a complex task such as locomoting throughout a dynamic environment requires not only the perception of various forms of information from the environment, but the integration of such information as to establish a more complete sensory experience. Visual perception, for example, relies not only on the visual system itself, but on the integration of the visual and vestibular systems. Perhaps the most well-known example of this integration is that of the vestibulo-ocular reflex, in which conjugate eye movements are reflexively bound to the detection of head motion by the vestibular system (Tresilian, 2012). This reflex can be easily elicited if one were to focus on keeping his or her gaze affixed to one point in space and moving the head; note that the retinal image will remain stable, as the movements of the eyes tend to counteract any otherwise disruptive movements of the head. This stabilizing capacity of the vestibular-ocular reflex is particularly important during locomotion, as will be discussed in the coming paragraphs.

In order to function properly, the vestibulo-ocular reflex requires a level of neuronal connectivity between the vestibular labyrinth and the musculature associated with eye movement. In an effort to describe the nature of this connectivity, the rotational vestibular-ocular reflex (associated with the semicircular canals) will be highlighted. In essence, the vestibular-ocular reflex is a complex circuit comprised of excitatory and inhibitory projections stemming from a particular semicircular canal to a particular ocular muscle (Leigh et al., 2015). If, for example, one is examining the vestibular-ocular reflex in the case of rotational head acceleration purely in the transverse plane, then one must look to the neuronal connections between the horizontal semicircular canal and the mediolateral recti

muscles. *Figure 2.13* (below, taken from Leigh et al., 2015) outlines the basic neuronal anatomy of the rotational vestibulo-ocular reflex by addressing each individual semicircular canal on the right side of the body and showing the path of connectivity between the canals, oculomotor neurons, and ocular muscles.

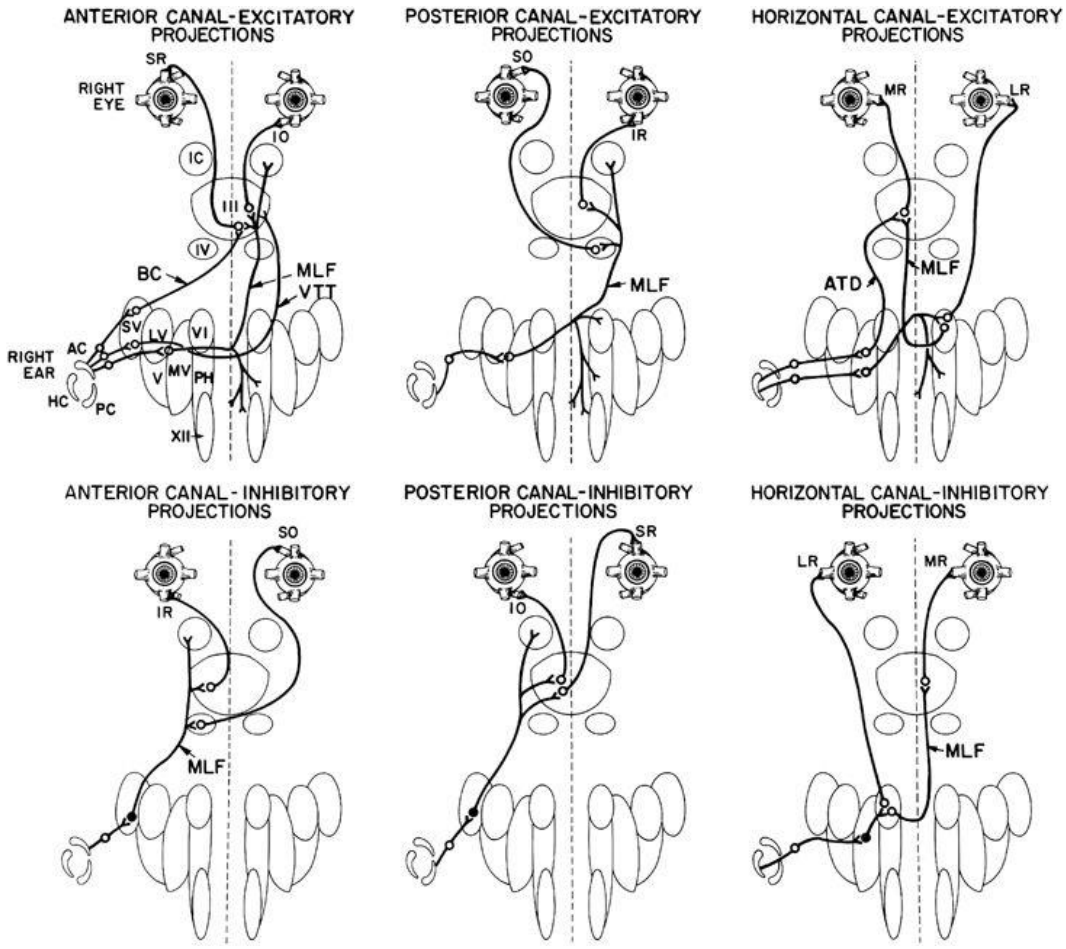

Figure 2.13 - Depiction of the neuronal connections comprising the vestibular-ocular reflex. Abbreviations: AC/PC/HC, anterior/posterior/horizontal canal; SR/MR/IR/LR, superior/medial/inferior/lateral rectus; SO/IO, superior/inferior oblique; III/IV/VI, third/fourth/sixth cranial nerve nucleus; IC, interstitial nucleus of Cajal; VTT, ventral tegmental tract; MLF, medial longitudinal fasciculus; ATD, ascending tract of Deiters; SV/LV/MV/V, superior/lateral/medial/inferior vestibular nucleus; BC, brachium conjunctivum; XII, hypoglossal nucleus; PH, prepositus hypoglossal nucleus - Figure taken from Leigh & Zee (2015).

Take, for example, the rotational acceleration that occurs in the transverse plane when the head is abruptly turned to the right. Here, one can see the relevant excitatory (top right image in *Figure 2.13*) and inhibitory (bottom right image) synaptic connections to the ocular muscles. In this specific case, the

left eye will be required to rotate laterally towards the temple, while the right eye will be required to rotate medially towards the nose if the retinal image is to be maintained. The neuronal connections responsible for this movement are illustrated in *Figure 2.13*, as the right semicircular canal is shown to inhibit the excitation of both the lateral rectus of the right eye and the medial rectus of the left eye. Note that the complete neuronal architecture of this reflex is far more intricate than a single excitatory or inhibitory connection to an individual muscle, as multiple synaptic connections are made with interneurons along the neuronal pathway (Leigh et al., 2015).

The capacity of the vestibulo-ocular reflex to mitigate perturbations to the retinal image is particularly beneficial during locomotion, as the accelerations resulting from ground contact might otherwise disrupt the visual field. Work from Borg et al.(Borg, Casanova, & Bootsma, 2015) affirmed this notion by examining the effects of the vestibulo-ocular reflex on visual perception in a variety of ecological conditions. Under natural conditions, for example, the information source is affixed to the environment itself. It is no surprise that these natural conditions are conducive to optimal visual function, as any small perturbation to the visual field resulting from head movement should be mitigated by the vestibulo-ocular reflex. In that sense, the vestibulo-ocular reflex evolved as a method for optimally perceiving information sources that are fixed to the environment. To further investigate the effects that various ecological conditions might have on visual perception, Borg et al. examined the differences in retinal image slip when the information source was fixed to 1) the environment and 2) the head of the participant. By disrupting the ecological conditions in which the vestibulo-ocular reflex was elicited, Borg et al. were able to demonstrate both its contribution to visual perception as well as its reflexive nature. Results from this experiment can be seen below in *Figure 2.14*.

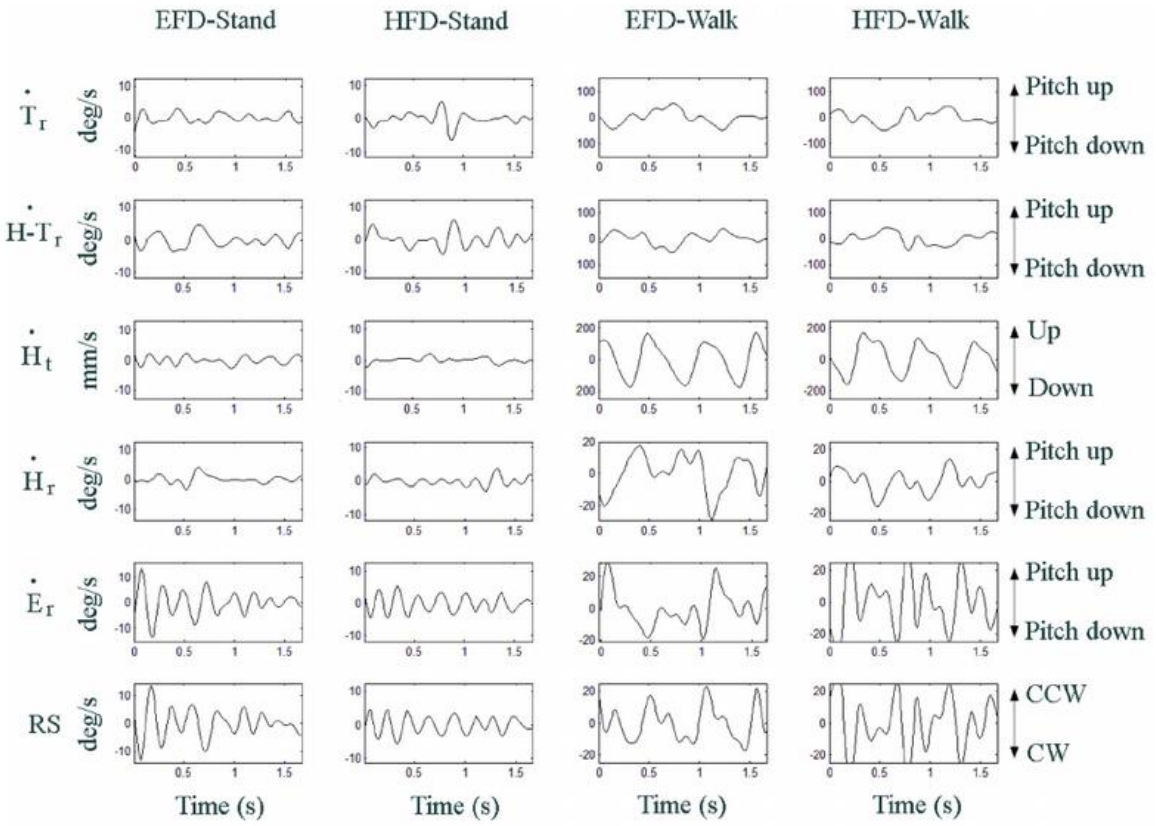

Figure 2.14 - From top to bottom: trunk rotation velocity, head-trunk rotation velocity, head translation velocity, head rotation velocity, eye rotation velocity and retinal slip. From left to right: earth-fixed display while standing, head-fixed display while standing, earth-fixed display while walking, head-fixed display while walking - Figure taken from Borg et al. (2015).

The vestibulo-ocular reflex is one of many examples of multisensory integration that is necessary for the optimal control of complex tasks such as bipedal locomotion. This reflex, while capable of mitigating the disruptive effects of ground impact forces during locomotion, is not alone responsible for the stabilization of the visual field in dynamic conditions. To account for the functional limitations of the vestibulo-ocular and vestibulo-collic reflexes, the locomotor system itself must adapt in an effort to mitigate the perturbing effects of locomotion (Hamill et al., 1995; Pulaski et al., 1981a; Wilson et al., n.d.). Indeed, the necessary integration of the locomotor, visuomotor, and vestibular systems underscores the immense complexity of everyday tasks that the human body is able to so effortlessly perform.

2.3.2 Head Stability

The deceleration of the musculoskeletal system resulting from ground-contact during human locomotion is an in inevitable product of the pendular dynamics discussed in section 2.2.1. This deceleration is typically accompanied by the transmission of the resultant shockwave through the system, thus potentially disrupting the stability of the visual field despite contributions from the vestibulo-ocular reflex (Derrick, Hamill, & Caldwell, 1998). To account for this, the locomotor system must adaptively attenuate the shock associated with ground contact as to afford optimal conditions for the function of the visual and vestibular systems. This affordance is ultimately the result of head stability, which was defined by Cromwell et al. in 2001 as the maintenance of head-in-space equilibrium (Cromwell, Newton, & Carlton, 2001). While the transmission of the shockwave imparted on the musculoskeletal system during the foot-ground collision is unavoidable, the magnitude of this collision is dependent upon locomotor parameters such as gait speed, stride frequency, and step length. Furthermore, the transmission of the shockwave imparted on the system is subject to attenuation by both passive and active structures that ultimately function to dissipate the energy of the shockwave by acting as a low-pass filter (Hamill et al., 1995). In this sense, head stability may be achieved by some combination of shock avoidance and shock attenuation.

In an effort to further elucidate the optimality criteria that define self-selected locomotor parameters, Hamill et al. (1995) assessed the relationship between stride frequency and shock attenuation in running. By constraining healthy participants to stride frequencies of 80%, 90%, 100%, 110%, and 120% of their preferred stride frequencies, Hamill et al. were able to examine what effect these imposed frequencies might have on shock attenuation, and whether shock attenuation appears to function as an optimality criterion. While shock attenuation itself did not appear to function as an optimality criterion, the results did uncover the tendency of the head to remain stable (that is, at a

constant level of acceleration), regardless of the magnitude of shockwave input (see *Table 2.1*)(Hamill et al., 1995).

Mean (*sd*) peak power spectral densities of leg and head accelerations

	Stride frequency				
	−20%	−10%	PSF	+10%	+20%
Leg					
Impact peak ($g^2 \cdot Hz^{-1}$)	0.1241	0.1140	0.0857	0.0641	0.0643
	(0.05)	(0.05)	(0.04)	(0.03)	(0.03)
Frequency of impact peak (Hz)	11.86	12.59	12.81	13.66	14.21
	(2.07)	(2.05)	(1.59)	(1.93)	(4.10)
Active peak ($g^2 \cdot Hz^{-1}$)	0.1058	0.0932	0.0776	0.0781	0.0708
	(0.054)	(0.034)	(0.026)	(0.024)	(0.029)
Frequency of active peak (Hz)	5.27	5.39	6.04	6.51	6.67
	(1.42)	(1.31)	(1.39)	(1.37)	(1.84)
Head					
Impact peak ($g^2 \cdot Hz^{-1}$)	0.0184	0.0186	0.0193	0.0188	0.0170
	(0.011)	(0.009)	(0.006)	(0.007)	(0.007)
Frequency of impact peak (Hz)	9.08	9.54	9.38	9.77	11.27
	(2.62)	(3.41)	(2.56)	(2.67)	(4.23)
Active peak ($g^2 \cdot Hz^{-1}$)	0.1761	0.1876	0.1712	0.1341	0.1068
	(0.079)	(0.070)	(0.060)	(0.053)	(0.045)
Frequency of peak (Hz)	2.99	3.10	3.47	3.75	4.04
	(0.70)	(0.74)	(0.58)	(0.68)	(0.70)

Table 2.1 - Accelerometer data collected from tibia and forehead during running at each of the five constrained stride frequencies - Table taken from Hamill et al. (1995).

Subsequent investigation by Derrick et al. (1998) sought to uncover the specific mechanisms by which shock is attenuated during locomotion (Derrick et al., 1998). While prior literature identified the role of passive structures in shock attenuation (Nigg, Cole, & Bruggemann, 1995), evidence underscoring the contribution of eccentric muscle contraction (Winter, 1983) provided the impetus for Derrick et al. to investigate the energy absorption at each joint across various stride lengths. Using a similar experimental protocol to Hamill et al. (1995), Derrick et al. (1998) constrained participants to stride lengths of 120%, 110%, 100%, 90%, and 80% of preferred stride length while participants ran at constant velocity. Accelerometers were affixed to the forehead and tibia as to measure shock attenuation, and joint moments were calculated using inverse dynamics. The negative work performed at each joint was calculated by integrating the joint power curves, and the amount of energy absorbed

was then compared across joints and stride lengths. Consistent with the results of Hamill et al. (1995), the total amount of shock attenuated by the body appeared to correlate with the amount of shock imparted on the system by the foot-ground collision, which serves to explain the tendency of the head to remain under constant acceleration. Furthermore, the results of Derrick et al. (1998) reveal each joint's capacity to absorb energy when locomotor parameters change, underscoring the adaptable nature of the system in its effort to maintain head stability during locomotion (Derrick et al., 1998).

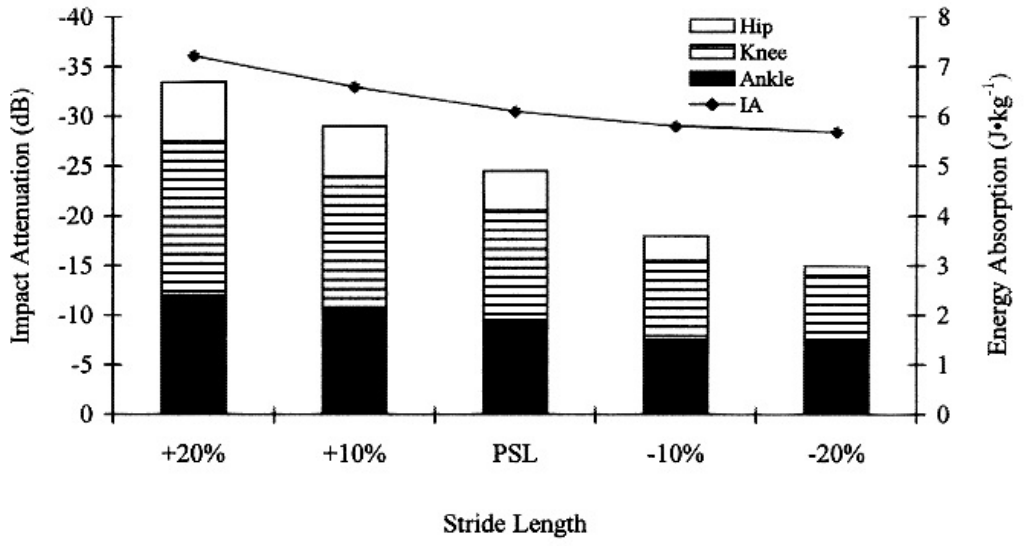

Figure 2.15 - Energy absorption at the hip, knee, and ankle joints across various stride lengths. Note that total impact attenuation is indicated by the line graph - Figure taken from Derrick et al. (1998).

More recent work by Lim et al. (2017) aimed to identify the role of imposed head stability requirements on running kinematics and shock attenuation (Lim, Busa, van Emmerik, & Hamill, 2017). By constraining the translational and rotational motion of the head during locomotion, Lim et al. were able to directly measure the kinematic parameters that contribute to head stability. Interestingly, when head stability demands were increased, no significant changes were found in the frequencies associated with the shockwave resulting from the food-ground collision (10-20 Hz). Rather, the changes in head stability seemed to result only from decreases in head acceleration during the active portion of

stance (associated with frequencies of 4-8 Hz), thus suggesting a voluntary kinematic adaptation. Furthermore, Lim et al. found that participants tended to increase stride frequency in response to increased head stability demands, underscoring the role of shock avoidance in the maintenance of head stability (Lim et al., 2017).

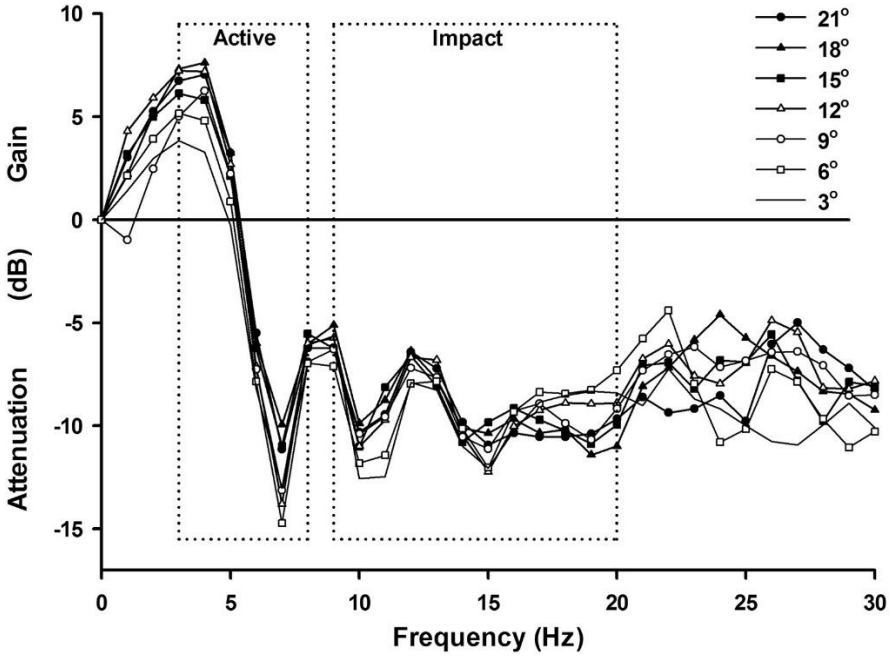

Figure 2.16 - Mean shock transfer functions between the tibia and forehead accelerations for all conditions (Note that a larger angle denotes an easier or less constrained stability task) - Figure taken from Lim et al. (2017).

Ultimately, achieving head stability during bipedal locomotion is a difficult task that requires a high degree of coordination between multiple complex systems within the body. While mechanisms such as the vestibulo-ocular reflex contribute to the stability of the visual field, their inherent limitations necessitate the mitigation of the perturbing accelerations associated with locomotion. The adaptive capacity of the locomotor system, then, is largely responsible for the relatively high levels of visual acuity experienced during running and walking (Borg et al., 2015).

2.3.3 Dynamic Visual Acuity

The human system is capable of effectively perceiving and acting upon visual information while locomoting through a dynamic environment. Such an ability requires, at the very least, the coordination of the visuomotor and locomotor systems. In turn, the visuomotor and locomotor systems themselves require the coordination of multiple constituent systems and processes. This nesting of biological systems, while necessary for the production of complex, adaptable movement, is relatively vulnerable to impairment when one or more constituent systems are disrupted. In this section, the effects of system disruption on dynamic visual acuity will be explored, as will the quantification of dynamic visual acuity itself.

Defined as the threshold of visual resolution obtained during relative motion of either optotype or observer (Miller & Ludvigh, 1962), dynamic visual acuity is of great relevance to both the clinical and research communities given the necessity of visual perception in daily life. Deficiencies in dynamic visual acuity, for example, may have lethal consequences when operating a vehicle or navigating a novel environment by foot (Cohen, 2006). Accordingly, (Hillman, Bloomberg, McDonald, & Cohen, 1999) chose to investigate the effects of vestibular deficiency on dynamic visual acuity by comparing the performance of healthy participants with those suffering from severe bilateral vestibular dysfunction. Participants afflicted by this pathology, referred to as *labyrinth-deficient patients* by Hillman et al., often reported a perturbing distortion of the visual field when moving the head or body through the environment. This sensation, originally defined as *oscillopsia* by Richard M. Brickner in 1963, has been the focus of much research by the national aeronautics and space administration (NASA) given its prevalence in post-flight astronauts and its potential impact on performance and mission success (Brickner, 1936; A. P. Mulavara & Bloomberg, 2002).

While much of the early literature on dynamic visual acuity dealt with optotypes moving horizontally from the reference frame of a static observer, Hillman et al. made an effort to not discount

the effects of shock transfer and locomotor behavior on visual perception by testing performance during treadmill walking (Hillman et al., 1999; Ludvigh, 1948). In line with their hypotheses, Hillman et al. found statistically significant differences between the dynamic visual acuity of healthy participants and labyrinth-deficient patients in both walking and standing conditions, despite the labyrinth-deficient patients having similar static visual acuity scores to the healthy participants. Similarly, the relative decrease in performance between the standing and walking conditions was found to be exacerbated in labyrinth deficient patients, suggesting that vestibular deficiency is particularly disruptive to visual field stability during locomotion (see *Figure 2.17*).

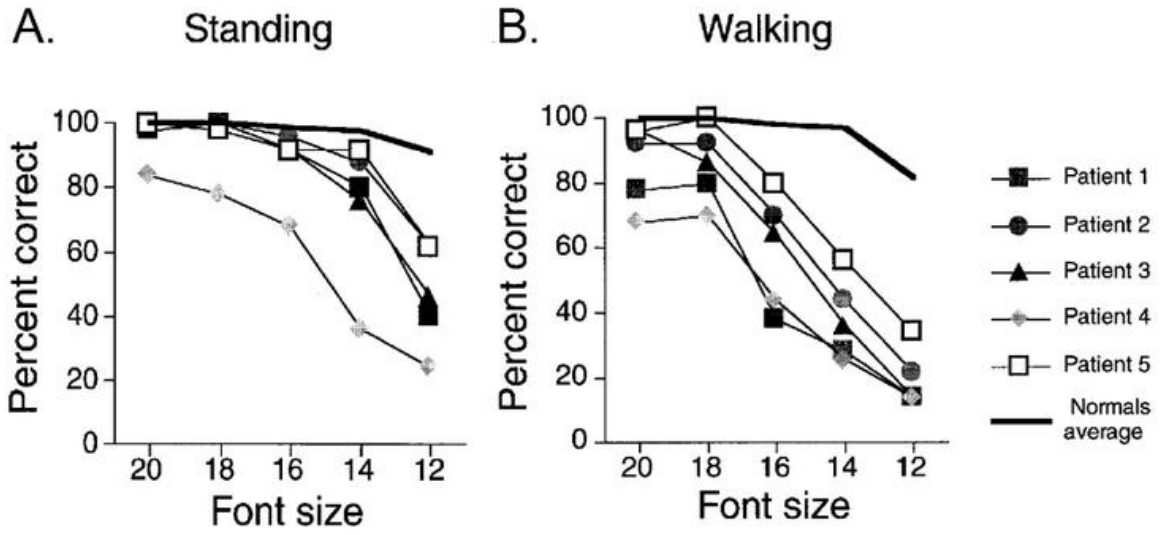

Figure 2.17 - Dynamic visual acuity performance in healthy and labyrinth deficient patients during standing and walking conditions - Figure taken from Hillman et al. (1999).

Following investigation by Hillman et al., Mulavara and Bloomberg (2002) aimed to identify the specific contributions of sensorimotor subsystem interactions in dynamic visual acuity following an increase in visual task demands during walking (A. P. Mulavara et al., 2002). Noting the relevance of coordination between 1) the eyes and the head, 2) the head and the trunk, and 3) the limbs and the environment, Mulavara and Bloomberg investigated how the aforementioned interactions would differ between a relatively simple visual task in which participants were instructed to focus on a central

target point (DOT) as opposed to when they were instructed to report projected numeral characters (NRT). The increase in visual task demands associated with the number recognition task was found to elicit significant changes to kinematic and kinetic parameters such as double support time, head pitch angle, knee flexion angle, and peak loading force. Double support time, for example, was found to have increased by ten percent following the increase in visual task demands; an adaptation that Mulavara and Bloomberg suggest might result in greater stability, therefore improving the participants' visual acuity during locomotion (A. P. Mulavara et al., 2002). Similarly, head pitch excursion kinematics were found to increase significantly in response to greater visual task demands despite no significant changes to trunk vertical or angular displacement (see *Table 2.2*). Further cross-correlation analysis by Mulavara and Bloomberg suggests that antiphase coupling of angular head motion and vertical trunk translation may contribute to visual field stability (A. P. Mulavara et al., 2002). Such coupling may serve to explain the relative increase in head motion seen when visual task demands increase, as the reflexive compensation in angular head motion may be augmented as to afford optimal conditions for visual perception.

	DOT	NRT
Head Pitch (deg)	2.96	3.63*
	(0.34)	(0.37)
Vertical Trunk Translation (mm)	53.80	56.10
	(2.54)	(6.02)
Trunk Pitch (deg)	2.82	2.74
	(0.23)	(0.20)
HPTP	0.57	0.59
	(0.01)	(0.02)
HPTV	−0.75	−0.78
	(0.03)	(0.02)

Table 2.2 - Group means of head pitch, vertical trunk translation, trunk pitch, the cross-correlation coefficient between head pitch and trunk pitch (HPTP), and the cross-correlation coefficient between head pitch and trunk vertical translation (HPTV). Note that all values are gathered from spectral curve integration between 1.5 and 2.5 Hz - Table taken from Mulavara and Bloomberg (2002).

With many of the reflexive and adaptive strategies implemented during increased visual task demands being mediated by the vestibular system, Peters and Bloomberg (2005) sought to disentangle the relative contributions of the otolith organs and semi-circular canals to dynamic visual acuity (Peters et al., 2005). Doing so was accomplished by assessing the relative decrements in dynamic visual acuity when participants transitioned from standing to walking during tasks in which they were instructed to report Landolt-C optotype orientations (see *Figure 2.18*) at distances of 0.5 and 4.0 meters. The increased parallax associated with "near" targets as opposed to "far" targets allowed for discrimination between deficiencies of the semicircular canals and otolith organs, as previous work demonstrated that the relative contribution of the otolith organs to the vestibulo-ocular reflex is dependent upon target distance (Snyder & King, 1996). Furthermore, Peters and Bloomberg note that the use of both "near" and "far" targets in dynamic visual acuity tests may serve as a particularly functional method of determining performance, given that target distances tend to be highly variable during tasks such as vehicle operation (Peters et al., 2005). To date, both "near" and "far" targets have been implemented by NASA in dynamic visual acuity assessments of the Expedition 11 crew (J. J. Mulavara et al., 2003).

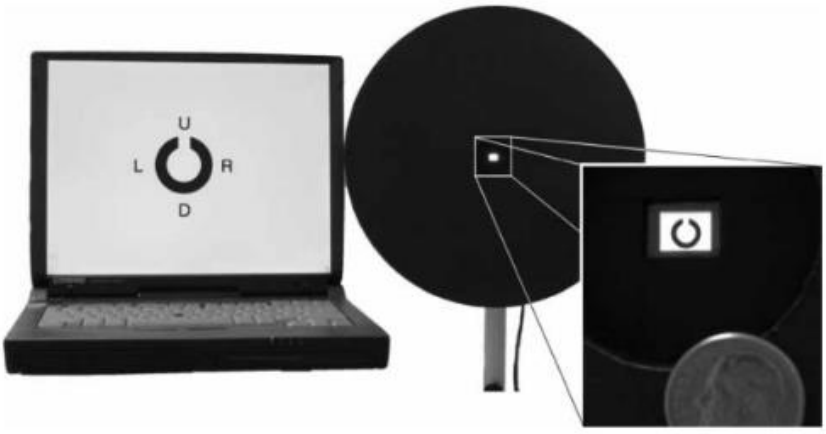

Figure 2.18 - Landolt-C optotype as projected on a laptop screen (used for the "far" target at a distance of 4.0 meters) and a microdisplay (used for the "near" target at a distance of 0.5 meters) - Figure taken from Peters and Bloomberg (2005).

In essence, dynamic visual acuity is a performance measure of the interaction of multiple nested systems that together give rise to optimal visual perception during locomotion. While it is easy to mistakenly attribute the entirety of visual perception to the eyes, one must remember the exploratory and dynamic nature of vision (Gibson, 1986). Visual field stability, for example, which is necessary for optimal dynamic visual acuity, is mediated largely by the interaction of the vestibular and visual systems (Borg et al., 2015). Likewise, head stability, which is necessary for optimal visual field stability, is mediated largely by the interaction of the locomotor system and the external environment (Lim et al., 2017). Despite the inherent redundancy of these interactions, disruption to one or more of the constituent systems often results in deficits to dynamic visual acuity. Such deficits may render a patient unable to safely operate a vehicle or navigate a novel environment, thus requiring rehabilitative measures targeting the afflicted systems (Cohen, 2006). Ultimately, the continued implementation and study of dynamic visual acuity is essential for the proper assessment of visual performance and for the further understanding of the requisite system interactions.

CHAPTER 3
METHODS

3.1 Participants

In this investigation, participants will be recruited from The University of Massachusetts Amherst. All participants will be required to provide informed consent in the form of written signature prior to participation. All procedures will be in accordance with the University of Massachusetts Institutional Review Board (IRB).

In addition to providing informed consent, all participants must meet the following inclusion criteria:

1) Participants must be between 18 and 40 years of age.
2) Participants must be free from any neurological or musculoskeletal impairment that may hinder the ability to locomote safely and efficiently.

3) Participants must possess 20/20 visual acuity. The use of corrective lenses is permissible, so long as the lenses are not bifocal.
4) Participants must respond in an acceptable manner to all questions listed on the Physical Activity Readiness Questionnaire (PAR-Q).

A sample size of 15 has been selected following a power analysis on prior work examining head stability under various visual task demands (Lim et al., 2017). It is expected that a sample size of 15 will be sufficient in determining statistical significance across the relevant parameters and conditions.

3.2 Equipment

3.2.1 Motion Capture

Kinematic data will be recorded using a four camera, high-speed, motion capture system (Oqus, Gothenburg, Sweden). This system will record the motion of 10 retroreflective markers placed bilaterally on the fifth metatarsal, lateral malleolus, fibular head, greater trochanter, and anterior superior iliac spine (ASIS) at 240 Hz.

3.2.2 Force Plates

Participants will be instructed to walk on a split-belt treadmill (Bertec, Columbus, Ohio) instrumented with force plates capable of measuring ground reaction forces in the vertical, anteroposterior, and mediolateral directions. A vertical ground reaction force threshold of 10 Newtons will be used to determine foot-ground contact. Ground reaction forces will be sampled at 1200 Hz.

3.2.3 Shock Attenuation

Tri-axial accelerometers (Delsys, Natick, Massachusetts) will be affixed to the forehead and the anteromedial distal aspect of the left and right tibiae (Hamill et al., 1995). To minimize artifact error,

each accelerometer will be secured with nylon straps and adjusted to the tolerance of each participant. Accelerations will be recorded in the vertical, anteroposterior, and mediolateral directions.

3.2.4 Visual Task

Landolt-C optotypes will be projected onto a screen in front of the split-belt treadmill during left heel strike. Optotype orientation will be generated randomly and constrained to four possible orientations: up, down, left, or right. Optotype size will be kept constant at 20/20 for all conditions.

3.3 Experimental Protocol

Participants will arrive at the Neuromechanics Laboratory at the University of Massachusetts Amherst and complete the Physical Activity Readiness Questionnaire. Assuming all inclusion criteria are met, participants will read and sign the Informed Consent Form as approved by the University Institutional Review Board. After providing informed consent, each participant will stand on the split-belt treadmill and verbally report the orientations of ten 20/20 Landolt-C optotypes. Each participant must report all ten optotype orientations correctly to continue. After screening participants for baseline visual acuity, retroreflective markers (see section 3.2.1) and tri-axial accelerometers (see section 3.2.3) will be affixed to the appropriate anatomical landmarks. Once retroreflective markers and accelerometers are in place, each participant will stand on the treadmill in anatomical position for a static reference trial.

During the *tied-belt baseline condition*, participants will walk on the treadmill in its tied-belt function at 1.8 m/s for ten minutes. During this condition, 20/20 Landolt-C optotypes will be projected with random orientation at left heel strike, and participants will report the perceived orientations verbally. Verbal reports will be recorded and scored for accuracy. Upon completing this condition, participants will rest for approximately one minute before continuing onto the adaptation condition.

During the *split-belt adaptation condition*, participants will walk on the treadmill in its split-belt function with the right belt set to travel and 0.6 m/s and the left belt set to travel at 1.8 m/s. Participants will be exposed to this 1:3 belt-speed ratio for ten minutes, during which the 20/20 Landolt-C optotypes will be projected with random orientation at left heel strike. Participants will be instructed to report optotype orientations verbally, and such reports will be recorded and scored for accuracy. Upon completing this condition, participants will rest for approximately one minute before continuing onto the washout condition.

During the *tied-belt washout condition,* participants will walk on the treadmill again in its tied-belt function at 1.8 m/s for ten minutes. During this condition, 20/20 Landolt-C optotypes will be projected with random orientation at left heel strike, and participants will report the perceived orientations verbally. Verbal reports will be recorded and scored for accuracy.

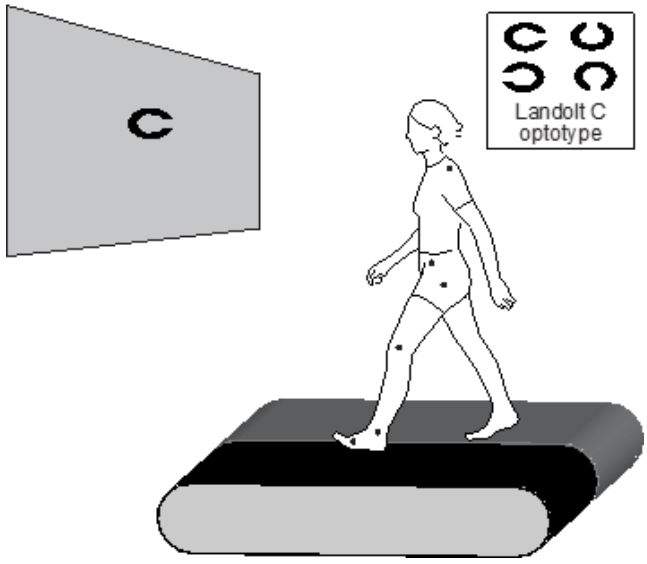

Figure 3.19 - Experimental task set-up, in which the Landolt-C optotype is projected on a screen in front of the split-belt treadmill - figure taken from "NSF Grant 2018 – Choi, Van Emmerik, & Hamill"

3.4 Data Analysis

3.4.1 Motion Capture

Kinematic data will be digitized using Qualysis Track Manager (Qualysis, Gothenburg, Sweden) before being processed with Visual 3D. All kinematic data will be treated with a low-pass, fourth-order Butterworth filter with a frequency cut-off determined by residual analysis (Lim et al., 2017). For all conditions (baseline, adaptation, and washout), step length asymmetry will be calculated by *equation 3.1*. In this equation, symmetrical step lengths will result in a value of zero, while step lengths of greater magnitude from left-to-right than from right-to-left will result in a positive value.

$$asym_L = \frac{l_{L\to R} - l_{R\to L}}{l_{L\to R} + l_{R\to L}}$$

Equation 3.1

Left-to-right step lengths will be calculated by *equation 3.2*, whereas right-to-left step lengths will be calculated by *equation 3.3*. In *equation 3.2,* step length is equal to the sum of 1) the anterior-posterior distance between the left and right lateral malleolus markers at right heel strike, and 2) the product of the left treadmill belt speed and the left to right step time.

$$l_{L\to R} = a_{L\to R} + v_L * t_{L\to R}$$

Equation 3.2

$$l_{R\to L} = a_{R\to L} + v_R * t_{R\to L}$$

Equation 3.2

3.4.2 Shock Attenuation

Tibial and head accelerometer data will be recorded continuously during all three conditions. Accelerometer data will be detrended and low-pass filtered using a dual-pass Butterworth filter with a frequency cutoff of 60 Hz (Hennig & Lafortune, 2016). A square window will be used to determine the

power spectral density of both the head and tibial accelerations during stance phase (Hamill et al., 1995). The impact phase for the tibia and head will be identified in both the temporal and frequency domains, occurring in the first 30% of stance and with a frequency range of 9 to 20 Hz. Likewise, the active phase for the tibia and head will occur in the latter 70% of stance with a frequency range of 3 to 8 Hz (Gruber, Boyer, Derrick, & Hamill, 2014a). Accordingly, the active and impact peaks will be identified as the peak acceleration values contained within each phase of stance. Signal power magnitudes for the impact and active phases will be calculated by integrating the signal powers within the previously described frequency ranges.

The transmission of acceleration from the tibia to the head may result in either shock gain or shock attenuation. The nature and magnitude of this transmission will be determined using the following transfer function (*equation 3.4)*, in which the power spectral density ratio between the tibia and head will be calculated across all relevant frequency bins (Hamill et al., 1995):

$$Transfer\ function\ (dB) = 10\ X\ log_{10}\left(\frac{PSD_{head}}{PSD_{tibia}}\right)$$

Equation 3.4

3.4.3 Dynamic Visual Acuity

Dynamic visual acuity performance will be defined by the percentage of accurately reported optotype orientations. An incorrectly reported optotype orientation will result in a score of zero, while a correctly reported optotype orientation will result in a score of one. Response times for optotype orientation will not be considered in determining dynamic visual acuity performance, as the repeated generation of optotypes with each stride will effectively impose a response time window.

3.5 Statistical Analysis

The effect of locomotor asymmetry on dynamic visual acuity performance will be assessed with analysis of variance (ANOVA). Locomotor asymmetry (1:1 and 1:3 belt-speed ratios) will serve as the independent variable, while dynamic visual acuity performance (correctly identified optotype orientations) will serve as the dependent variable.

The effects of locomotor asymmetry on head stability and shock attenuation will be assessed with analysis of variance (ANOVA). Locomotor asymmetry (1:1 and 1:3 belt-speed ratios) will serve as the independent variable, while head stability and shock attenuation (defined by *equation 3.4*) will serve as the dependent variables.

The nature of visuomotor adaptation during imposed locomotor asymmetry will be assessed with a polynomial regression analysis. This analysis will examine changes in dynamic visual acuity performance throughout the three conditions.

CHAPTER 4
MANUSCRIPT

4.1 Abstract

Necessary for effective ambulation, head stability affords optimal conditions for the perception of visual information during dynamic tasks. This maintenance of head-in-space equilibrium is achieved, in part, by the attenuation of the high frequency impact shock resulting from ground contact. While a great deal of experimentation has been done on the matter during steady state locomotion, little is known about how head stability or dynamic visual acuity is maintained during asymmetric walking.

In this study, fifteen participants were instructed to walk on a split-belt treadmill for ten minutes while verbally reporting the orientation of a randomized Landolt-C optotype that was projected at heel strike. Participants were exposed to the baseline, adaptation, and washout conditions, as characterized by belt speed ratios of 1:1, 1:3, and 1:1, respectively. Step length asymmetry, shock attenuation, high (impact)

and low (active) frequency head signal power, and dynamic visual acuity scores were averaged across the first and last fifty strides of each condition.

Over the course of the first fifty strides, step length asymmetry was significantly greater during adaptation than during baseline (p <0.001; d =2.442). Additionally, high frequency head signal power was significantly greater during adaptation than during baseline (p <0.001; d =1.227), indicating a reduction in head stability. Shock attenuation was significantly lower during adaptation than during baseline (p <0.05; d =-0.679), and a medium effect size suggests that dynamic visual acuity was lower during adaptation than during baseline as well (p =0.052; d =0.653). When comparing the baseline and adaptation conditions across the last fifty strides, however, many of these decrements were greatly reduced.

The results of this study indicate that the locomotor asymmetry imposed by the split-belt treadmill during the early adaptation condition is responsible for moderate decrements to shock attenuation, head stability, and dynamic visual acuity. Moreover, the relative reduction in magnitude of these decrements across the last fifty strides underscores the adaptive nature of the locomotor and visuomotor systems.

4.2 Introduction

In order for an organism to interact with its environment in a manner that is both stable and adaptable, the organism must prioritize the perception of environmental information. In humans, even the most mundane of tasks (e.g., quiet standing) are subject to perturbation provided environmental information is either removed or sufficiently distorted (David N. Lee & Aronson, 1974). Early experimentation by Lee and Aronson on the role of visual proprioception in infants, in which compensatory ankle torque was observed in response to an illusory optic flow, is perhaps the most powerful and well-known illustration of this phenomenon (David N. Lee et al., 1974). The tendency of the human system to respond in

indistinguishable manner to perturbations that are based either in information (e.g., optic flow) or in energy (e.g., moving platform) should serve to underscore how intimately the two domains are bound in the context of the human-environment system (Hughes, Schenkman, Chandler, & Studenski, 1995; David N. Lee et al., 1974). It is a logical conclusion, then, that the study of human locomotion ought to consider the ways in which human movement might optimize not only the actions of the organism, but the concurrent perception of environmental information as well.

During locomotion, ground contact is accompanied by the propagation of a shockwave through the musculoskeletal system towards the head, thus potentially disrupting the visual field (Hamill et al., 1995). While the vestibulo-ocular reflex (VOR) is able to mitigate the perturbation associated with ground contact, its effectiveness is limited to a relatively low range of rotational velocities (Pulaski, Zee, & Robinson, 1981b). To account for this, the locomotor system must adaptively attenuate the shockwave as to afford optimal conditions for the function of both the visual and vestibular systems. Though the impartation and subsequent transmission of this shockwave is unavoidable, the magnitude of the collision is dependent upon locomotor parameters such as gait speed, stride frequency, and step length (Derrick et al., 1998; Hamill et al., 1995; Mercer et al., 2010). Furthermore, the shockwave itself is subject to attenuation by both passive and active mechanisms which function to dissipate the energy of the signal by acting as a low-pass filter (Hamill et al., 1995). In this sense, head stability, and therefore visual field stability, may be achieved by some combination of shock avoidance and shock attenuation. Interestingly, the degree to which the shockwave is attenuated during steady state locomotion appears proportionate to the magnitude of the impact shock (Hamill et al., 1995). In other words, the maintenance of head-in-space equilibrium appears nearly invariant to shockwave input (Cromwell et al., 2001). Evidence supporting this claim can be found in a number of experiments in which participants have been methodologically constrained in gait speed, stride frequency, or stride length (Derrick et al., 1998; Hamill et al., 1995; Mercer et al., 2010). Such constraints have resulted in the modulation of shock

attenuation by the musculoskeletal system, ultimately resulting in an invariantly stable head during early stance. While the tendency of the musculoskeletal system to stabilize the head during dynamic tasks is clear, the biomechanical mechanisms by which this is accomplished are nontrivial. Prior investigation on the attenuation of impact shock has classified the relevant dissipative mechanisms into two distinct categories. The first category, which includes all passive mechanisms, is the result of muscle tissue oscillation and mechanical deformation occurring in the shoe, heel pad, and ligaments (De Clercq, Aerts, & Kunnen, 1994; Paul et al., 1978; Shorten, Valiant, & Cooper, 1986). The second category, including all active mechanisms, is the result of alterations in gait dynamics which lead to an increase in energy absorption along the kinetic chain (Gruber, Boyer, Derrick, & Hamill, 2014b). Further research has implicated increased knee flexion, reduced pronation of the foot, and increased muscle activation in the upper and lower body as the primary mechanisms by which impact shock is actively attenuated (Boyer & Nigg, 2004; Cromwell et al., 2001; Kavanagh, Barrett, & Morrison, 2006; Paul et al., 1978).

Despite numerous experiments having considered the ways in which head stability might be affected by altered gait parameters, very few have considered the converse; that is whether such alterations might be adopted by the locomotor system in response to explicit head stability demands. Recent investigation on the matter has revealed that when head stability demands are increased during running, stride frequency tends to increase, and the magnitude and integrated power of low frequency head accelerations are minimized (Lim et al., 2017). These changes suggest that the locomotor system is able to modulate the vertical displacement of the head during the propulsive phase of stance, which may further aid in visual perception.

The tendency of the locomotor system to optimize head stability under a number of conditions suggests that further investigation into visual perception and locomotion is warranted, and that such investigation should be restricted neither to running nor to steady state walking. The imposition of locomotor asymmetry by use of a split-belt treadmill has allowed for both detailed analysis of locomotor

adaptation, as well as for precise manipulation of ecological complexity via asymmetry (Selgrade, Toney, & Chang, 2017). Common use of the split-belt paradigm consists of exposing the participants first to the treadmill in its tied-belt state, where both belts move jointly as they would on a conventional treadmill. Following this baseline condition, the speeds of the treadmill belts diverge, and the participant is instructed to walk for several minutes while one limb moves two or three times faster than the other (Torres-Oviedo et al., 2011). Upon initial exposure to this adaptation condition, participants experience decrements to interlimb coordination characterized by asymmetrical step lengths and step times (D. S. Reisman et al., 2005). As exposure continues, the locomotor system adapts, and these gait parameters shift towards baseline symmetry. When the treadmill is returned to its tied-belt function during the subsequent washout condition, healthy participants typically experience a loss of symmetry mirroring that which occurs during the adaptation condition, indicating that a degree of motor adaptation has occurred (Roemmich et al., 2018). Despite the pervasiveness of this paradigm in the current biomechanical and neurophysiological literature, no studies have considered how head stability might be achieved or maintained during the three conditions. Moreover, the effect that imposed locomotor asymmetry might have on the perception of visual information is unknown.

Accordingly, this paper aims to assess whether the locomotor asymmetry commonly observed during the split-belt paradigm might result in decrements to shock attenuation and head stability, and whether these proposed decrements might then result in a reduced capacity to accurately perceive visual information. It was hypothesized that 1) the locomotor asymmetry associated with the adaptation and washout conditions will result in reduced shock attenuation (Roemmich et al., 2018), 2) any reduction in shock attenuation will lead to a decrease in head stability (Hamill et al., 1995), and 3) any reduction in head stability will lead to a decreased ability to accurately perceive visual information (Cromwell et al., 2001).

4.3 Methods

4.3.1 Participants

Fifteen participants (10 females, 5 males; 24.67 +/- 4.67 years of age; 69.60 +/- 12.59 kg) were recruited for this study. All participants were free from neurological and musculoskeletal impairment at the time of collection. Participants responded in an acceptable manner to all questions listed on the Physical Activity Readiness Questionnaire (PAR-Q) and provided informed consent in the form of written signature prior to collection. All procedures were approved by the University of Massachusetts Institutional Review Board.

4.3.2 Apparatus

Retroreflective markers were placed bilaterally on the head, trunk, pelvis, and lower extremities (Fig. 1A). Kinematic data were recorded at 100 Hz with eight Miqus M3 infrared cameras (Qualisys, Gothenburg, Sweden).

Delsys Trigno Inertial Measurement Units (IMUs) (Delsys, Natick, Massachusetts) were placed bilaterally on the anteromedial distal aspect of the tibiae, as well as on the frontal bone. IMUs were securely fastened to subject tolerance prior to collection. IMUs were synchronized with Qualisys Track Manager (Qualisys, Gothenburg, Sweden) and sampled at 2000 Hz.

Ground reaction forces were collected at 2000 Hz using an instrumented split-belt treadmill (Bertec, Columbus, OH). A vertical ground reaction force threshold of 10 Newtons was used to determine foot-ground contact.

Landolt-C optotypes were projected onto a high-definition monitor located approximately two meters in front of the treadmill. Optotypes were projected for 700 ms every other left heel strike using a custom

written MatLab program (The MathWorks, Natick, MA) (Fig. 1B). Optotype orientation was randomized prior to projection, and verbal responses were recorded on a personal computer.

4.3.3 Experimental protocol

Participants were instructed to stand in anatomical position on the split-belt treadmill for a static calibration trial lasting 10 s. Upon completion of the static calibration trial, participants were instructed to verbally report the orientation of several Landolt-C optotypes while walking at 1.2 m/s. Optotype size was then modified by the experimenter until correct identification by the participant was between 50 and 75 percent for no less than 20 consecutive responses. This range of identification success was determined during pilot testing to elicit the greatest sensitivity to the three walking conditions. Participants were first exposed to the baseline condition, where both belts traveled at 1.2 m/s for ten minutes. Following the baseline condition, participants were exposed to the adaptation condition, where the right belt traveled at 1.8 m/s and the left belt traveled at 0.6 m/s for ten minutes. Following the adaptation condition, participants were exposed to the washout condition, where both belts traveled again at 1.2 m/s for ten minutes. Participants were permitted to rest for approximately two minutes between each condition.

Landolt-C optotypes were projected with random orientation every other left heel strike, and participants were instructed to report the orientations verbally for each condition.

4.3.4 Data Analysis

Kinematic data were filtered using a fourth-order, zero-lag, low-pass Butterworth digital filter with a cutoff frequency of 6 Hz. Right and left step lengths were defined as the anteroposterior distance between the two lateral malleoli at right and left heel strike, respectively. Heel strike was identified

using the anteroposterior positional data of the malleoli. Step length asymmetry was computed across five hundred consecutive strides by the following equation, where SL_R is right step length and SL_L is left step length (Smith & Martin, 2007):

$$SL_{asym} = \frac{SL_R - SL_L}{0.5 * (SL_R + SL_L)} \quad \text{(Eq. 1)}$$

Accelerometry data were filtered using a second-order, zero-lag, low-pass Butterworth digital filter with a cutoff frequency of 40 Hz. Power spectral densities were computed from the vertical accelerometer profiles of the head and tibiae across one thousand consecutive stance phases using the Welch's power spectral density estimate (pwelch) function in MatLab. Note that stance was defined as heel strike to contralateral heel strike rather than to ipsilateral toe off in order to maintain only one impact peak per stance phase. Gait events were identified on the vertical accelerometer profiles of the tibiae using a custom written MatLab program, as an inter-system delay rendered kinematic and force plate data untenable in the identification of gait events in the accelerometry data.

Vertical acceleration signal power values were then computed by independently integrating the power spectral densities within both the high (9-20 Hz) and low (1-8 Hz) frequency ranges associated with ground contact and active propulsion, respectively (Lim et al., 2017). Note that while these frequency ranges have been most commonly used in experiments on running, the delineation between high and low frequency appears consistent across forms of locomotion (James, Mileva, & Cook, 2014).

The gain or attenuation of vertical acceleration amplitude between the tibiae and the head at each 1 Hz frequency bin during stance was then computed using the following transfer function, where PSD_{head} is the power spectral density of the head during stance, and PSD_{tibia} is the power spectral density of the tibia during stance (Hamill et al., 1995):

$$Amplitude = 10 \text{ x } log_{10} \ (PSD_{head}/PSD_{tibia}) \quad \text{(Eq. 2)}$$

High frequency attenuation was then defined as the sum of all negative amplitudes within the high frequency range associated with ground contact (9-20 Hz) (Fig. 2).

Verbal responses to optotype orientation were scored as either correct or incorrect across five hundred consecutive strides, and dynamic visual acuity was defined as the average correctness of the responses.

4.3.5 Statistical Analysis

All dependent measures were averaged across the first and last fifty strides of each condition in order to capture any effect of motor adaptation (Fig. 3). Repeated measures analyses of variance (ANOVA) were then performed on each dependent measure to examine the effect of condition at early and late time intervals. Greenhouse-Geisser corrections were applied in any instance where the assumption of sphericity was violated (p <0.05). *Post hoc* pairwise comparisons were performed using *t*-tests, to which Bonferroni adjustments were applied. In addition to *p* values, effect sizes were reported in order to illustrate the magnitude of any statistical differences.

Paired samples *t*-tests were also used to assess the condition-specific differences between early and late dependent measures in all cases where the assumption of normality was not violated. In cases where the assumption of normality *was* violated (Shapiro-Wilk; p <0.05), Wilcoxon signed rank tests were instead used. While effect size is typically given by matched rank biserial correlation for Wilcoxon signed rank tests, all effect sizes listed in Table 2 are given by Cohen's *d* to allow for more direct comparison. In converting biserial correlation to Cohen's *d*, the following equation was used, in which *r* is the biserial correlation (Fritz, Morris, & Richler, 2012):

$$d = \frac{2r}{\sqrt{(1-r^2)}} \qquad \text{(Eq. 3)}$$

A significance threshold of α =0.05 was used for all inferential statistics. Effect size ranges for Cohen's *d* were small (0.20), moderate (0.50), and large (0.80). All statistical analyses were performed using JASP (JASP, Amsterdam, The Netherlands).

4.4 Results

4.4.1 Step Length Asymmetry

There was a significant main effect of condition on step length asymmetry across both the first (p <0.001) and last (p <0.001) fifty strides, as indicated in Table 1. *Post hoc* analysis further revealed that step length asymmetry was greater in both the adaptation (p <0.001; d =2.442) and washout (p =0.006; d =-0.876) conditions than in the baseline condition across the first fifty strides (Table 2A; Fig. 4). Across the last fifty strides, *post hoc* analysis revealed that step length asymmetry was greater in the adaptation condition than in the baseline condition (p <.001; d =1.648), though no difference was found to exist between the baseline and washout conditions (p >0.05; d = -0.201) (Table 2B; Fig. 4).
Step length asymmetry was found to decrease from the first to the last fifty strides within both the adaptation (p <0.001; d =-1.927) and washout (p <0.001; d =-1.000) conditions, but not within the baseline condition (p >0.05; d =-0.307) (Table 3; Fig. 4).

4.4.2 Shock Attenuation

There was no significant main effect of condition on shock attenuation across either the first (p =0.058) or last (p =0.343) fifty strides (Table 1). It is worth noting, however, that shock attenuation was significantly lower in the adaptation condition than in the baseline condition across the first fifty strides, as revealed by *post hoc* analysis (p <0.05; d =-0.679) (Table 2A; Fig. 4).

No significant differences were found to exist between early and late shock attenuation values in any of the three conditions (p >0.05), though a small effect of exposure suggests a potential decrease in the measure across the baseline condition (p =0.080; d =-0.488) (Table 3; Fig. 4).

4.4.3 Impact Head Power

There was a significant main effect of condition on impact head power across both the first (p <0.001) and last (p <0.05) fifty strides (Table 1). *Post hoc* analysis further revealed that impact head power was significantly higher in the adaptation condition than in both the baseline (p <0.001; d =-1.227) and washout (p <0.05; d =0.883) conditions across the first fifty strides (Table 2A; Fig. 4). Across the last fifty strides, *post hoc* analysis revealed that impact head power was again higher in the adaptation condition than in both the baseline (p <0.05; d =-0.959) and washout (p <0.05; d =0.776) conditions (Table 2B; Fig. 4).

No significant differences were found to exist between early and late values of impact head power for either the adaptation (p =0.075; d =0.393) or washout (p >0.05; d =-0.060) conditions, though a small effect of exposure in the adaptation condition suggests a potential decrease in the measure. Interestingly, a significant increase in impact head power was found across the baseline condition (p <0.05; d =-2.155) (Table 3; Fig. 4).

4.4.4 Active Head Power

A significant main effect of condition was found on active head power across both the first (p <0.05) and last (p <0.01) fifty strides (Table 1). *Post hoc* analysis further revealed that active head power was significantly higher in the adaptation condition than in both the baseline (p <0.05; d =-0.901) and washout (p <0.05; d =0.851) conditions across the first fifty strides (Table 2A; Fig. 4). Similar results were

found across the last fifty strides, with active head power again being significantly higher in the adaptation condition than in both the baseline (p <0.001; d =-1.116) and washout (p <0.05; d =1.011) conditions (Table 2B; Fig. 4).

No significant differences were found between early and late values of active head power in any of the three conditions (p >0.05), though a large effect of exposure was found within the baseline condition, suggesting a potential increase in the measure (p =0.055; d =-1.377) (Table 3; Fig. 4).

4.4.5 Dynamic Visual Acuity

There was no significant main effect of condition on dynamic visual acuity across either the first (p =0.052) or last (p =0.480) fifty strides (Table 1). It is worth noting, however, that a medium effect of condition was revealed in the *post hoc* analysis, suggesting that dynamic visual acuity was lower in the adaptation condition than in the baseline condition across the first fifty strides (p =0.052; d =0.653) (Table 2A; Fig. 4).

Dynamic visual acuity was found to increase significantly from the first to the last fifty strides in the adaptation condition (p <0.05; d =-0.520). No significant differences were observed within either the baseline or washout conditions, though a small effect of exposure suggests a potential increase in the measure during the washout condition (p =0.074; d =-0.394).

4.5 Discussion

The purpose of this study was to assess whether the locomotor asymmetry commonly observed during the split-belt paradigm might result in decrements to shock attenuation and head stability, and whether these decrements might then result in reduced dynamic visual acuity. It was hypothesized that 1) the locomotor asymmetry associated with the adaptation and washout conditions would result in reduced

shock attenuation, 2) any reduction in shock attenuation would lead to an increase in head signal power, and 3) any increase in head signal power would lead to a reduction in dynamic visual acuity. When comparing the baseline and adaptation conditions across the first fifty strides, all dependent measures followed their hypothesized trends, with step length asymmetry, impact head power, and active head power being higher in the adaptation condition than in the baseline condition, and shock attenuation and dynamic visual acuity being lower in the adaptation condition than in the baseline condition (Table 2A; Fig. 4). These decrements suggest that the locomotor asymmetry resulting from exposure to the split-belt treadmill is sufficient in its perturbing effect to disrupt the capacity of the locomotor system to attenuate impact shock, thereby leading to a decrease in head stability and dynamic visual acuity.

Many of the decrements that were observed between the baseline and adaptation conditions across the first fifty strides appear to have been attenuated by the last fifty strides. The increase in step length asymmetry between the two conditions, for example, was larger across the first fifty strides than across the last fifty strides (Table 2; Fig. 4). Likewise, shock attenuation and dynamic visual acuity, while both being significantly lower in the adaptation condition than in the baseline condition across the first fifty strides, were not significantly different between the two conditions across the last fifty strides (Table 2; Fig. 4). Though it is tempting to attribute the relative mitigation of these decrements to the locomotor adaptation occurring in the adaptation condition, this does not always appear to be the case. The absence of any baseline-adaptation differences in shock attenuation across the last fifty strides, for example, is not due to an increase in shock attenuation across the adaptation condition, but rather to a decrease in the measure across the baseline condition (Table 3; Fig. 4). Interestingly, these results differ from prior literature, which suggests that shock attenuation is often prioritized during steady state locomotion, even in the absence of a visual task (Hamill et al., 1995; Ratcliffe & Holt, 1997).

Another interesting result is the apparent discrepancy between dynamic visual acuity and shock attenuation across the adaptation condition, in which dynamic visual acuity, but not shock attenuation,

increased from the first to the last fifty strides of the condition (Table 3B; Fig. 4). Such a discrepancy suggests that the locomotor system might employ a number of different strategies to maintain dynamic visual acuity, as an increase in the measure need not be achieved solely by an increase in shock attenuation. One such strategy might be the adoption of a locomotor pattern that prioritizes the avoidance rather than the attenuation of impact shock, as high frequency head power depends both on the magnitude of the shockwave imparted on the system as well as on the attenuation thereof (Hamill et al., 1995). If, for example, less impact shock is imparted on the musculoskeletal system during ground contact, then less attenuation would be required to achieve the same degree of high frequency head power. Indeed, the adoption of such a pattern is a plausible explanation for the discrepancy seen here, as a small reduction in high frequency head power was observed from the first to the last fifty strides of the condition (Table 3B; Fig. 4).

In contrast to the observed reduction in high frequency head power, low frequency head power appeared to increase from the first to the last fifty strides in the adaptation condition, as indicated by a moderate effect size (Table 3B; Fig. 4). While such a result was not expected, it is not surprising that a strategy of active head modulation might be employed by individuals performing a visual task. Adoption of such a strategy is consistent with prior literature, as results by Lim et al. suggest that active head modulation in the 4-8 Hz range is one mechanism by which head stability might be achieved during locomotion (Lim et al., 2017). It is worth noting, however, that individuals in the study by Lim et al. were tasked only with minimizing head motion, while individuals in this present study were tasked with accurately reporting the orientation of an optotype. As a result, the active head modulation observed in the study by Lim et al. resulted in a decrease in low frequency head power in response to increased head stability demands, while the active head modulation observed in this present study resulted in an increase in low frequency head power across the adaptation condition. Though it cannot be said with certainty why an increase in active head power was observed, it is possible that individuals in this

present study adapted to both the environmental constraints and to the visual task by increasing compensatory head motion, leading to an increase in dynamic visual acuity (Pozzo, Berthoz, & Lefort, 1990).

While all dependent measures followed their hypothesized trends between the early baseline and adaptation conditions, step length asymmetry was the only measure to do so between the early baseline and washout conditions. Indeed, no significant decrements in shock attenuation, impact head signal power, active head signal power, or dynamic visual acuity were observed between the two conditions across the first fifty strides (Table 2A; Fig. 4). These results, while in contradiction to the stated hypotheses, might provide insight into the degree to which the locomotor system must be challenged before any downstream decrements are observed. As step length asymmetry was significantly lower in the washout condition than in the adaptation condition across the first fifty strides, it is possible that the degree of asymmetry exhibited by the locomotor system in the early washout condition failed to reach some threshold required to produce observable decrements in shock attenuation, head stability, and dynamic visual acuity. Moreover, while no decrements in these downstream measures were of statistical significance, all measures were directionally in accordance with their hypothesized trends (Table 2A; Fig. 4). It is therefore plausible that if the degree of locomotor asymmetry observed in the early washout condition were higher, decrements in shock attenuation, head stability, and dynamic visual acuity would have been observed.

In sum, the results of this study suggest that the locomotor asymmetry imposed by the split-belt treadmill is sufficient in its perturbing effect to elicit decrements in shock attenuation, head stability, and dynamic visual acuity. Moreover, the tendency of these decrements to appear commensurate with the degree of locomotor asymmetry should further underscore the coupling of the locomotor and visuomotor systems. As indicated earlier, however, the maintenance of dynamic visual acuity cannot be thought to represent the degree to which any one strategy or reflex is being utilized. Indeed, the

redundant nature of the locomotor system permits not only a high degree of dynamic visual acuity, but a wide array of strategies to be employed in the maintenance thereof. Specifically, it appears that shock attenuation, shock avoidance, and active head modulation are all mechanisms by which the perception of visual information is optimized during locomotion. The results presented here provide novel insights into the relationship of the locomotor and visuomotor systems, particularly when the former is challenged by environmental perturbation. Future research in this area should explore, more thoroughly, the role of active head motion in the perception of visual information.

4.6 Conflicts of Interest

The authors have no conflicts of interest to declare.

4.7 Tables:

Table 1A
Repeated measures analyses of variance to determine the effect of condition on step length (SL) asymmetry, shock attenuation, impact head power, active head power, and dynamic visual acuity (DVA) across the first fifty strides. Note that the shock attenuation, impact head power, and active head power values are during left stance, only.

Measure (Early)	Sphericity Correction	Sum of Squares	df	Mean Square	F	p
SL Asymmetry	Greenhouse-Geisser	3.480	1.201	2.898	88.742	< .001
Shock Attenuation	Greenhouse-Geisser	12513.009	1.437	8707.241	3.639	0.058
Impact Head Power	None	5.104e -4	2.000	2.552e -4	12.026	< .001
Active Head Power	Greenhouse-Geisser	0.006	1.157	0.005	7.692	0.011
DVA Score	None	0.093	2.000	0.046	3.304	0.052

Table 1B
Repeated measures analyses of variance to determine the effect of condition on step length asymmetry, shock attenuation, impact head power, active head power, and dynamic visual acuity across the last fifty strides. Note that the below shock attenuation, impact head power, and active head power values are during left stance, only.

Measure (Late)	Sphericity Correction	Sum of Squares	df	Mean Square	F	p
SL Asymmetry	Greenhouse-Geisser	0.463	1.020	0.453	30.874	< .001
Shock Attenuation	None	3954.701	2.000	1977.350	1.114	0.343
Impact Head Power	None	2.990e -4	2.000	1.495e -4	7.774	0.002
Active Head Power	Greenhouse-Geisser	0.017	1.174	0.014	11.398	0.003
DVA Score	Greenhouse-Geisser	0.016	1.448	0.011	0.660	0.480

Table 2A
Post Hoc Comparisons – Condition (first fifty strides)

Early SL Asymmetry		**Mean Difference**	**SE**	**t**	**Cohen's d**	**p_{bonf}**
Baseline	Adaptation	0.484	0.051	9.460	2.442	< .001
Baseline	Washout	-0.174	0.051	-3.394	-0.876	0.006
Adaptation	Washout	-0.657	0.051	-12.854	-3.319	< .001
Early Shock Attenuation		**Mean Difference**	**SE**	**t**	**Cohen's d**	**p_{bonf}**
Baseline	Adaptation	-39.836	15.140	-2.631	-0.679	0.041
Baseline	Washout	-27.735	15.140	-1.832	-0.473	0.233
Adaptation	Washout	12.102	15.140	0.799	0.206	1.000
Early Head Impact Power		**Mean Difference**	**SE**	**t**	**Cohen's d**	**p_{bonf}**
Baseline	Adaptation	-0.008	0.002	-4.754	-1.227	< .001
Baseline	Washout	-0.002	0.002	-1.332	-0.344	0.581
Adaptation	Washout	0.006	0.002	3.422	0.883	0.006
Early Head Active Power		**Mean Difference**	**SE**	**t**	**Cohen's d**	**p_{bonf}**
Baseline	Adaptation	-0.025	0.007	-3.489	-0.901	0.005
Baseline	Washout	-0.001	0.007	-0.192	-0.050	1.000
Adaptation	Washout	0.023	0.007	3.297	0.851	0.008
Early DVA Score		**Mean Difference**	**SE**	**t**	**Cohen's d**	**p_{bonf}**
Baseline	Adaptation	0.109	0.043	2.528	0.653	0.052
Baseline	Washout	0.037	0.043	0.863	0.223	1.000
Adaptation	Washout	-0.072	0.043	-1.665	-0.430	0.321

Note. Cohen's d does not correct for multiple comparisons.
Note. P-value adjusted for comparing a family of 3

Table 2B
Post Hoc Comparisons – Condition (last fifty strides)

Late SL Asymmetry		**Mean Difference**	**SE**	**t**	**Cohen's d**	**p_{bonf}**
Baseline	Adaptation	0.202	0.032	6.382	1.648	< .001
Baseline	Washout	-0.025	0.032	-0.779	-0.201	1.000
Adaptation	Washout	-0.226	0.032	-7.161	-1.849	< .001
Late Shock Attenuation		**Mean Difference**	**SE**	**t**	**Cohen's d**	**p_{bonf}**
Baseline	Adaptation	-22.615	15.387	-1.470	-0.379	0.458
Baseline	Washout	-14.754	15.387	-0.959	-0.248	1.000
Adaptation	Washout	7.861	15.387	0.511	0.132	1.000
Late Head Impact Power		**Mean Difference**	**SE**	**t**	**Cohen's d**	**p_{bonf}**
Baseline	Adaptation	-0.006	0.002	-3.713	-0.959	0.003
Baseline	Washout	-0.001	0.002	-0.707	-0.183	1.000
Adaptation	Washout	0.005	0.002	3.006	0.776	0.017
Late Head Active Power		**Mean Difference**	**SE**	**t**	**Cohen's d**	**p_{bonf}**
Baseline	Adaptation	-0.043	0.010	-4.324	-1.116	< .001
Baseline	Washout	-0.004	0.010	-0.408	-0.105	1.000
Adaptation	Washout	0.039	0.010	3.916	1.011	0.002
Late DVA Score		**Mean Difference**	**SE**	**t**	**Cohen's d**	**p_{bonf}**
Baseline	Adaptation	0.016	0.040	0.400	0.103	1.000
Baseline	Washout	-0.029	0.040	-0.733	-0.189	1.000
Adaptation	Washout	-0.045	0.040	-1.133	-0.293	0.800

Note. Cohen's d does not correct for multiple comparisons.
Note. P-value adjusted for comparing a family of 3

Table 3A
Step length asymmetry, shock attenuation, impact head power, active head power, and dynamic visual acuity scores across the first fifty (early) and last fifty (late) strides during the *baseline condition*. Note that the below shock attenuation, impact head power, and active head power values are during left stance, only.

Early Baseline		Late Baseline	Test	Statistic	df	p	Location Parameter	SE Difference	Effect Size
SL Asymmetry	-	SL Asymmetry	*t*-test	1.189	14	0.254	0.006	0.005	0.307
Shock Attenuation	-	Shock Attenuation	*t*-test	-1.888	14	0.080	-16.686	8.837	-0.488
Impact Head Power	-	Impact Head Power	Wilcoxon	16.000	-	0.010	-0.001	-	-2.155
Active Head Power	-	Active Head Power	Wilcoxon	26.000	-	0.055	-7.884e -4	-	-1.377
DVA Score	-	DVA Score	*t*-test	-0.174	14	0.864	-0.008	0.046	-0.045

Note. For the Student t-test, location parameter is given by mean difference. For the Wilcoxon test, location parameter is given by the Hodges-Lehmann estimate.

Table 3B
Step length asymmetry, shock attenuation, impact head power, active head power, and dynamic visual acuity scores across the first fifty (early) and last fifty (late) strides during the *adaptation condition*. Note that the below shock attenuation, impact head power, and active head power values are during left stance, only.

Early Adaptation		Late Adaptation	Test	Statistic	df	p	Location Parameter	SE Difference	Effect Size
SL Asymmetry	-	SL Asymmetry	*t*-test	-7.464	14	<0.001	-0.276	0.037	-1.927
Shock Attenuation	-	Shock Attenuation	Wilcoxon	62.000	-	0.467	0.358	-	0.066
Impact Head Power	-	Impact Head Power	*t*-test	1.520	14	0.075	7.447e -4	4.898e -4	0.393
Active Head Power	-	Active Head Power	*t*-test	-2.447	14	0.986	-0.020	0.008	-0.632
DVA Score	-	DVA Score	*t*-test	-2.053	14	0.030	-0.101	0.049	-0.530

Note. For the Student t-test, location parameter is given by mean difference. For the Wilcoxon test, location parameter is given by the Hodges-Lehmann estimate.

Table 3C
Step length asymmetry, shock attenuation, impact head power, active head power, and dynamic visual acuity scores across the first fifty (early) and last fifty (late) strides during the *washout condition*. Note that the below shock attenuation, impact head power, and active head power values are during left stance, only.

Early Washout		Late Washout	Test	Statistic	df	p	Location Parameter	SE Difference	Effect Size
SL Asymmetry	-	SL Asymmetry	Wilcoxon	120.000	-	<0.001	0.133	-	1.000*
Shock Attenuation	-	Shock Attenuation	*t*-test	-0.366	14	0.640	-3.705	10.129	-0.094
Impact Head Power	-	Impact Head Power	*t*-test	-0.233	14	0.591	-1.978e -4	8.482e -4	-0.060
Active Head Power	-	Active Head Power	Wilcoxon	58.000	-	0.555	-8.643e -5	-	-0.066
DVA Score	-	DVA Score	*t*-test	-1.527	14	0.074	-0.075	0.049	-0.394

Note. For the Student t-test, location parameter is given by mean difference. For the Wilcoxon test, location parameter is given by the Hodges-Lehmann estimate.
* Effect size is given by the matched rank biserial correlation, as conversion to Cohen's d is not possible with an *r* of 1.0 when using Eq. 3.

4.8 Figure Captions:

Fig. 1: Retro-reflective marker set (A): Markers were placed on the head (1a – 1d), acromia (2), iliac crests (3), anterior superior iliac spines (4), posterior superior iliac spines (5), sacrum (6), greater trochanters (7), thighs (8; four-marker rigid clusters), medial and lateral epicondyles (9), shanks (10; four-marker rigid clusters), medial and lateral malleoli (11), and on the shoes (12a – 13). Markers shown in grey were attached for the calibration trial, only. Markers shown with crosshairs in the front view are attached on the posterior side of the body. Figure adapted from (Lim et al., 2017).

Experimental setup (B): Landolt-C optotypes were projected at left heel strike onto a high-definition monitor located approximately two meters in front of the split-belt treadmill. The orientation of each optotype was randomized prior to projection.

Fig. 2: Derivation of head signal power and high frequency attenuation. As shown, vertical accelerations at the tibia and head were normalized to percent stance. Using the Welch's power spectral density estimate (pwelch) function in MatLab, these normalized acceleration profiles were then converted into their respective power spectral densities, from which low and high head signal power values were computed. Finally, with the transfer function shown in Eq. (2), these power spectral densities were used to derive the attenuation of high frequency power between the tibia and head during stance.

Fig. 3: Group means for each dependent measure across the three conditions. Note that the vertical lines in each subplot indicate the end of the early and the start of the late values.

Fig. 4: Early and late values of each dependent measure across the three conditions. Note that absolute values are plotted to allow for more direct comparison of magnitudes across the measures.

4.9 Figures:

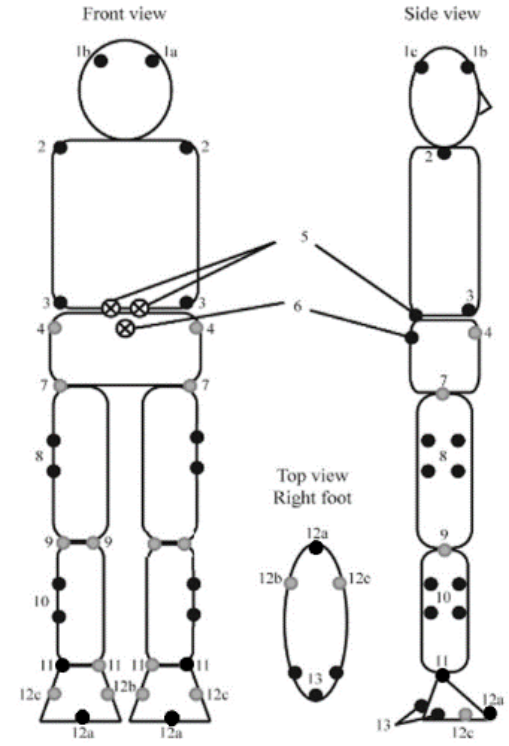

Fig. 1A

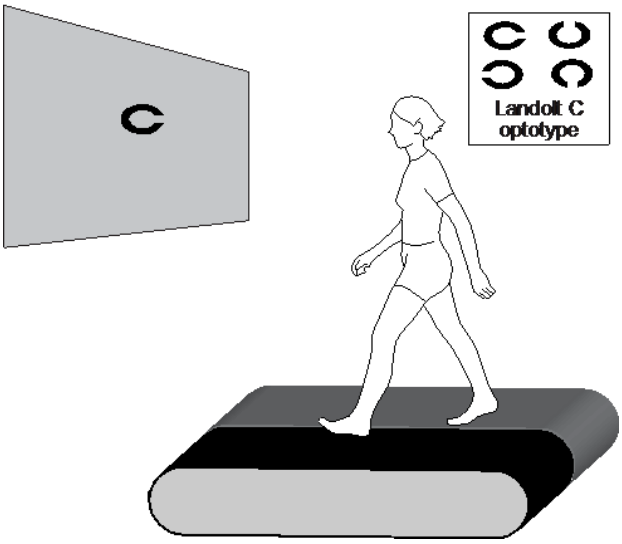

Fig. 1A

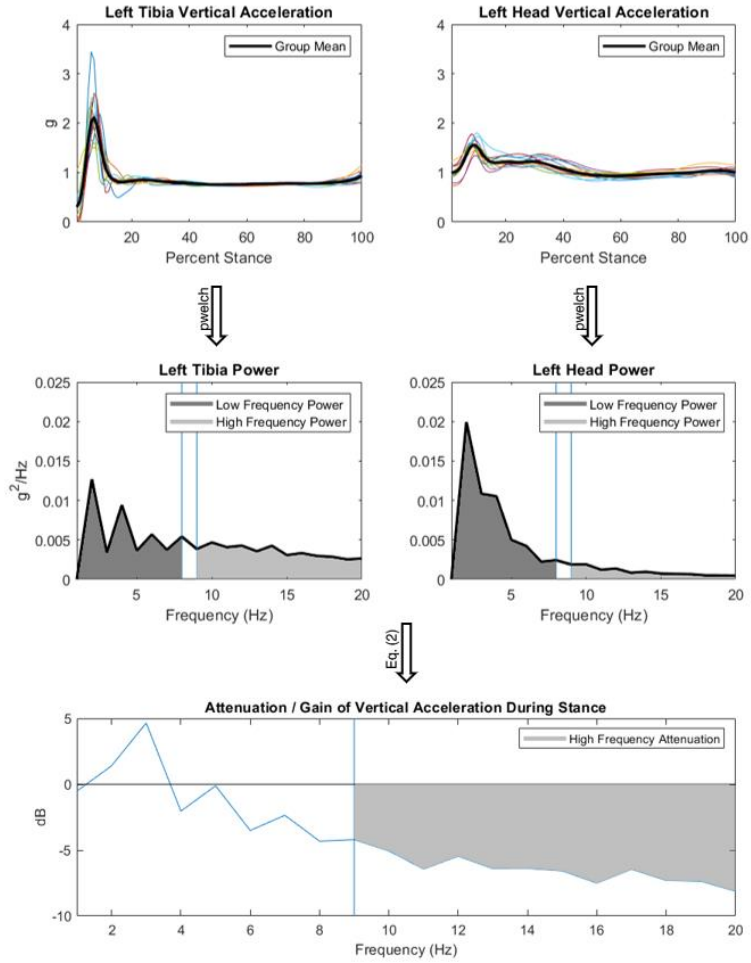
Left Tibia Vertical Acceleration
Group Mean
g
Percent Stance
Left Head Vertical Acceleration
Group Mean
Percent Stance
pwelch
pwelch
Left Tibia Power
Low Frequency Power
High Frequency Power
g²/Hz
Frequency (Hz)
Left Head Power
Low Frequency Power
High Frequency Power
Frequency (Hz)
Eq. (2)
Attenuation / Gain of Vertical Acceleration During Stance
High Frequency Attenuation
dB
Frequency (Hz)

Fig. 2

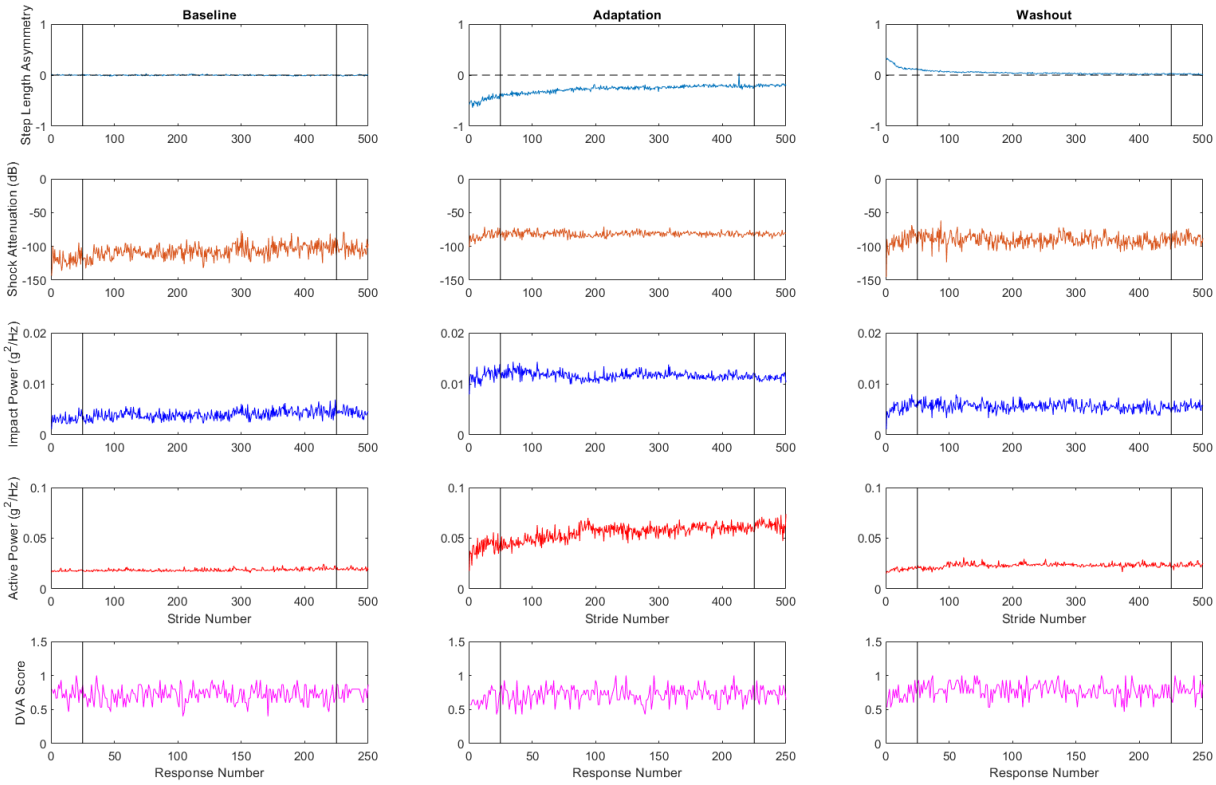
Baseline
Adaptation
Washout
Step Length Asymmetry
Shock Attenuation (dB)
Impact Power (g²/Hz)
Active Power (g²/Hz)
DVA Score
Stride Number
Response Number

Fig. 3

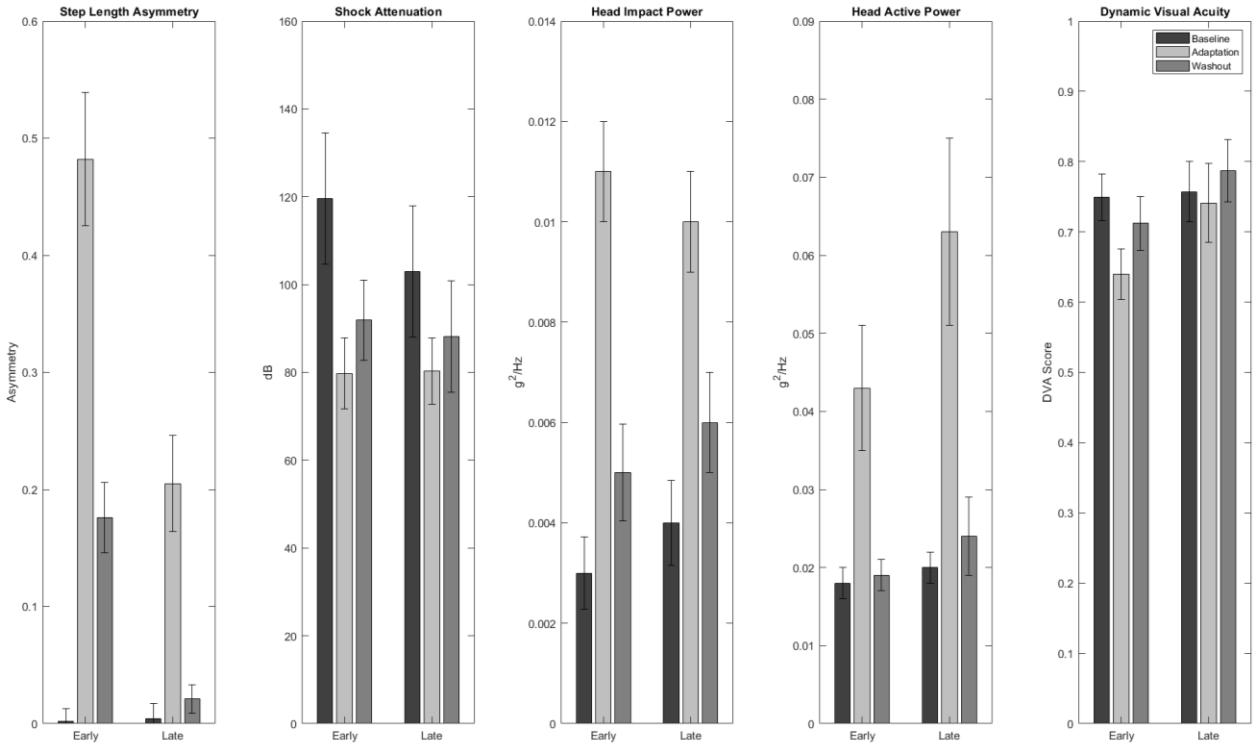
Step Length Asymmetry
Asymmetry
Early
Late
Shock Attenuation
dB
Early
Late
Head Impact Power
g²/Hz
Early
Late
Head Active Power
g²/Hz
Early
Late
Dynamic Visual Acuity
DVA Score
Baseline
Adaptation
Washout
Early
Late

Fig. 4

REFERENCES

Borg, O., Casanova, R., & Bootsma, R. J. (2015). Reading from a Head-Fixed Display during Walking: Adverse Effects of Gaze Stabilization Mechanisms. *PLOS ONE*, *10*(6), e0129902. https://doi.org/10.1371/journal.pone.0129902

Boyer, K. A., & Nigg, B. M. (2004). Muscle activity in the leg is tuned in response to impact force characteristics. *Journal of Biomechanics*, *37*(10), 1583–1588. https://doi.org/10.1016/j.jbiomech.2004.01.002

Brickner, R. M. (1936). Oscillopsia: A new symptom commonly occurring in multiple sclerosis. *Archives of Neurology And Psychiatry*, *36*(3), 586–589. https://doi.org/10.1001/archneurpsyc.1936.02260090139009

Cohen, H. S. (2006). Disability and rehabilitation in the dizzy patient. In *Current Opinion in Neurology*. https://doi.org/10.1097/01.wco.0000194373.08203.33

Cromwell, R. L., Newton, R. A., & Carlton, L. G. (2001). Horizontal plane head stabilization during locomotor tasks. *Journal of Motor Behavior*, *33*(1), 49–58. https://doi.org/10.1080/00222890109601902

De Clercq, D., Aerts, P., & Kunnen, M. (1994). The mechanical characteristics of the human heel pad during foot strike in running: An in vivo cineradiographic study. *Journal of Biomechanics*, *27*(10), 1213–1222. https://doi.org/10.1016/0021-9290(94)90275-5

Derrick, T. R., Hamill, J., & Caldwell, G. E. (1998). Energy absorption of impacts during running at various stride lengths. *Medicine and Science in Sports and Exercise*, *30*(1), 128–135. https://doi.org/10.1097/00005768-199801000-00018

Descartes, R., Cottingham, J., Stoothoff, R., Murdoch, D., Descartes, R., Cottingham, J., Stoothoff, R., & Murdoch, D. (2012). The Passions of the Soul. In *The Philosophical Writings of Descartes*. https://doi.org/10.1017/cbo9780511805042.010

Dickinson, M. H., Farley, C. T., Full, R. J., Koehl, M. A. R., Kram, R., Lehman, S., T, F. C., J, F. R., A, K. M., R, K., & S, L. (2000). How animals move: An integrative view. *Science*, *288*(5463), 100–106. https://doi.org/10.1126/science.288.5463.100

Dietz, V., Zijlstra, W., & Duysens, J. (1994). Human neuronal interlimb coordination during split-belt locomotion. *Experimental Brain Research*, *101*(3), 513–520. https://doi.org/10.1007/BF00227344

Dimitrijevic, M. R., Gerasimenko, Y., & Pinter, M. M. (1998). Evidence for a spinal central pattern generator in humans. *Annals of the New York Academy of Sciences*, *860*, 360–376. https://doi.org/10.1111/j.1749-6632.1998.tb09062.x

Einstein, A. (1920). Sidelights on Relativity: ETHER AND THE THEORY OF RELATIVITY and GEOMETRY AND EXPERIENCE. In *Report*.

Finley, J. M., & Bastian, A. J. (2017). Associations between Foot Placement Asymmetries and Metabolic Cost of Transport in Hemiparetic Gait. *Neurorehabilitation and Neural Repair*, *31*(2), 168–177. https://doi.org/10.1177/1545968316675428

Finley, J. M., Bastian, A. J., & Gottschall, J. S. (2013). Learning to be economical: The energy cost of walking tracks motor adaptation. *Journal of Physiology*, *591*(4), 1081–1095. https://doi.org/10.1113/jphysiol.2012.245506

Forgaard, C. J., Franks, I. M., Maslovat, D., & Chua, R. (2016). Perturbation predictability can influence the long-latency stretch response. *PLoS ONE*, *11*(10). https://doi.org/10.1371/journal.pone.0163854

Frigon, A., Johnson, M. D., & Heckman, C. J. (2011). Altered activation patterns by triceps surae stretch reflex pathways in acute and chronic spinal cord injury. *Journal of Neurophysiology*, *106*(4), 1669–1678. https://doi.org/10.1152/jn.00504.2011

Chapter 16 Functional plasticity following spinal cord lesions, 157 Progress in Brain Research 231 (2006). https://doi.org/10.1016/S0079-6123(06)57016-5

Fritz, C. O., Morris, P. E., & Richler, J. J. (2012). Effect size estimates: Current use, calculations, and interpretation. *Journal of Experimental Psychology: General*, *141*(1), 2–18. https://doi.org/10.1037/a0024338

Gibson, J. J. (1950). *The perception of the visual world*. Houghton Mifflin.

Gibson, J. J. (1986). The Ecological Approach to Visual Perception. In *of Experimental Psychology Human Perception and*.

Gruber, A. H., Boyer, K. A., Derrick, T. R., & Hamill, J. (2014a). Impact shock frequency components and attenuation in rearfoot and forefoot running. *Journal of Sport and Health Science*, *3*(2), 113–121. https://doi.org/10.1016/j.jshs.2014.03.004

Gruber, A. H., Boyer, K. A., Derrick, T. R., & Hamill, J. (2014b). Impact shock frequency components and attenuation in rearfoot and forefoot running. *Journal of Sport and Health Science*, *3*(2), 113–121. https://doi.org/10.1016/j.jshs.2014.03.004

Hamill, J., Derrick, T. R., & Holt, K. G. (1995). Shock attenuation and stride frequency during running. *Human Movement Science*, *14*(1), 45–60. https://doi.org/10.1016/0167-9457(95)00004-C

Heeck, J. (2013). How stable is the photon? *Physical Review Letters*, *111*(2). https://doi.org/10.1103/PhysRevLett.111.021801

Hennig, E. M., & Lafortune, M. A. (2016). Relationships between Ground Reaction Force and Tibial Bone Acceleration Parameters. *International Journal of Sport Biomechanics*. https://doi.org/10.1123/ijsb.7.3.303

Hillman, E. J., Bloomberg, J. J., McDonald, P. V, & Cohen, H. S. (1999). Dynamic visual acuity while walking in normals and labyrinthine-deficient patients. *Journal of Vestibular Research : Equilibrium & Orientation*, *9*(1), 49–57. http://www.ncbi.nlm.nih.gov/pubmed/10334016

Holt, K. G., Hamill, J., & Andres, R. O. (1991). Predicting the minimal energy costs of human walking. *Medicine and Science in Sports and Exercise*, *23*(4), 491–498. https://doi.org/10.1249/00005768-

199104000-00016

Hooper, S. L., & Marder, E. (1987). Modulation of the lobster pyloric rhythm by the peptide proctolin. *Journal of Neuroscience*, *7*(7), 2097–2112. https://doi.org/10.1523/jneurosci.07-07-02097.1987

Houck, J. R., Duncan, A., & Haven, K. E. D. (2006). Comparison of frontal plane trunk kinematics and hip and knee moments during anticipated and unanticipated walking and side step cutting tasks. *Gait and Posture*, *24*(3), 314–322. https://doi.org/10.1016/j.gaitpost.2005.10.005

Hughes, M. A., Schenkman, M. L., Chandler, J. M., & Studenski, S. A. (1995). Postural responses to platform perturbation: kinematics and electromyography. *Clinical Biomechanics*, *10*(6), 318–322. https://doi.org/10.1016/0268-0033(94)00001-N

James, D. C., Mileva, K. N., & Cook, D. P. (2014). Low-frequency accelerations over-estimate impact-related shock during walking. *Journal of Electromyography and Kinesiology*, *24*(2), 264–270. https://doi.org/10.1016/j.jelekin.2013.12.008

Kandel, E.; Schwartz, J.; Jessel, T. M. (1991). *Principles of Neural Science, Fifth Edition | AccessNeurology | McGraw-Hill Medical*. Elsevier,.

Kavanagh, J., Barrett, R., & Morrison, S. (2006). The role of the neck and trunk in facilitating head stability during walking. *Experimental Brain Research*, *172*(4), 454–463. https://doi.org/10.1007/s00221-006-0353-6

Kuo, A. D. (2007). The six determinants of gait and the inverted pendulum analogy: A dynamic walking perspective. *Human Movement Science*, *26*(4), 617–656. https://doi.org/10.1016/j.humov.2007.04.003

Kuo, A. D., Donelan, J. M., & Ruina, A. (2005). Energetic consequences of walking like an inverted pendulum: Step-to-step transitions. *Exercise and Sport Sciences Reviews*, *33*(2), 88–97. https://doi.org/10.1097/00003677-200504000-00006

Lee, D. N. (1976). A theory of visual control of braking based on information about time to collision.

Perception, *5*(4), 437–459. https://doi.org/10.1068/p050437

Lee, David N., & Aronson, E. (1974). Visual proprioceptive control of standing in human infants. *Perception & Psychophysics*, *15*(3), 529–532. https://doi.org/10.3758/BF03199297

Lee, David N., & Reddish, P. E. (1981). Plummeting gannets: A paradigm of ecological optics. *Nature*, *293*(5830), 293–294. https://doi.org/10.1038/293293a0

Leigh, R. J., & Zee, D. S. (2015). The Neurology of Eye Movements. In *The Neurology of Eye Movements*. https://doi.org/10.1093/med/9780199969289.001.0001

Liddell, E. G. T., & Sherrington, C. (1924). Reflexes in Response to Stretch (Myotatic Reflexes). *Proceedings of the Royal Society B: Biological Sciences*, *96*(675), 212–242. https://doi.org/10.1098/rspb.1924.0023

Lim, J., Busa, M. A., van Emmerik, R. E. A., & Hamill, J. (2017). Adaptive changes in running kinematics as a function of head stability demands and their effect on shock transmission. *Journal of Biomechanics*, *52*, 122–129. https://doi.org/10.1016/j.jbiomech.2016.12.020

Ludvigh, E. (1948). The visibility of moving objects. *Science*, *108*(2794), 63–64. https://doi.org/10.1126/science.108.2794.63

Malone, L. A., & Bastian, A. J. (2010). Thinking about walking: Effects of conscious correction versus distraction on locomotor adaptation. *Journal of Neurophysiology*, *103*(4), 1954–1962. https://doi.org/10.1152/jn.00832.2009

Marder, E., & Bucher, D. (2001). Central pattern generators and the control of rhythmic movements. *Current Biology*, *11*(23). https://doi.org/10.1016/S0960-9822(01)00581-4

Matthews, P. B. C. C. (1991). The human stretch reflex and the motor cortex. *Trends in Neurosciences*, *14*(3), 87–91. https://doi.org/10.1016/0166-2236(91)90064-2

McLean, D. L., Masino, M. A., Koh, I. Y. Y., Lindquist, W. B., & Fetcho, J. R. (2008). Continuous shifts in the active set of spinal interneurons during changes in locomotor speed. *Nature Neuroscience*, *11*(12),

1419–1429. https://doi.org/10.1038/nn.2225

Mercer, J. A., Dufek, J. S., Mangus, B. C., Rubley, M. D., Bhanot, K., & Aldridge, J. M. (2010). A description of shock attenuation for children running. *Journal of Athletic Training*, *45*(3), 259–264. https://doi.org/10.4085/1062-6050-45.3.259

MILLER, J. W., & LUDVIGH, E. (1962). The effect of relative motion on visual acuity. *Survey of Ophthalmology*, *7*, 83–116. http://www.ncbi.nlm.nih.gov/pubmed/14474056

Morton, S. M., & Bastian, A. J. (2006). Cerebellar contributions to locomotor adaptations during splitbelt treadmill walking. *Journal of Neuroscience*, *26*(36), 9107–9116. https://doi.org/10.1523/JNEUROSCI.2622-06.2006

Mulavara, A. P., & Bloomberg, J. J. (2002). Identifying head-trunk and lower limb contributions to gaze stabilization during locomotion. *Journal of Vestibular Research: Equilibrium and Orientation*, *12*(5–6), 255–269.

Mulavara, J. J., Mulavara, A. P., Bloomberg, A. P., Peters, J. J., Bloomberg, B. T., & Otoluryngol, J. J. (2003). INTEGRATED LOCOMOTOR FUNCTION TESTS FOR COUNTERMEASURE EVALUATION. In *IEEE Engineering in Medicine andBiology Mugmine* (Vol. 22, Issue 2). In Press. https://ntrs.nasa.gov/search.jsp?R=20060024888

Nigg, B. M., Cole, G. K., & Bruggemann, G. P. (1995). Impact forces during heel-toe running. *Journal of Applied Biomechanics*. https://doi.org/10.1123/jab.11.4.407

Patla, A. E., Adkin, A., & Ballard, T. (1999). Online steering: Coordination and control of body center of mass, head and body reorientation. *Experimental Brain Research*, *129*(4), 629–634. https://doi.org/10.1007/s002210050932

Paul, I. L., Munro, M. B., Abernethy, P. J., Simon, S. R., Radin, E. L., & Rose, R. M. (1978). Musculo-skeletal shock absorption: Relative contribution of bone and soft tissues at various frequencies. *Journal of Biomechanics*, *11*(5), 237–239. https://doi.org/10.1016/0021-9290(78)90049-0

Peters, B. T., & Bloomberg, J. J. (2005). Dynamic visual acuity using “far” and “near” targets. *Acta Oto-Laryngologica*, *125*(4), 353–357. https://doi.org/10.1080/00016480410024631

Pozzo, T., Berthoz, A., & Lefort, L. (1990). Head stabilization during various locomotor tasks in humans - I. Normal subjects. *Experimental Brain Research*, *82*(1), 97–106. https://doi.org/10.1007/BF00230842

Pulaski, P. D., Zee, D. S., & Robinson, D. A. (1981a). The behavior of the vestibulo-ocular reflex at high velocities of head rotation. *Brain Research*, *222*(1), 159–165. https://doi.org/10.1016/0006-8993(81)90952-5

Pulaski, P. D., Zee, D. S., & Robinson, D. A. (1981b). The behavior of the vestibulo-ocular reflex at high velocities of head rotation. *Brain Research*, *222*(1), 159–165. https://doi.org/10.1016/0006-8993(81)90952-5

Ratcliffe, R. J., & Holt, K. G. (1997). Low frequency shock absorption in human walking. *Gait and Posture*, *5*(2), 93–100. https://doi.org/10.1016/S0966-6362(96)01077-6

Reisman, D., Kesar, T., Perumal, R., Roos, M., Rudolph, K., Higginson, J., Helm, E., & Binder-Macleod, S. (2013). Time course of functional and biomechanical improvements during a gait training intervention in persons with chronic stroke. *Journal of Neurologic Physical Therapy*, *37*(4), 159–165. https://doi.org/10.1097/NPT.0000000000000020

Reisman, D. S., Block, H. J., & Bastian, A. J. (2005). Interlimb coordination during locomotion: What can be adapted and stored? *Journal of Neurophysiology*, *94*(4), 2403–2415. https://doi.org/10.1152/jn.00089.2005

Reisman, D. S., Wityk, R., Silver, K., & Bastian, A. J. (2007). Locomotor adaptation on a split-belt treadmill can improve walking symmetry post-stroke. *Brain*, *130*(7), 1861–1872. https://doi.org/10.1093/brain/awm035

Roemmich, R. T., & Bastian, A. J. (2018). Closing the Loop: From Motor Neuroscience to

Neurorehabilitation. *Annual Review of Neuroscience*, *41*(1), 415–429. https://doi.org/10.1146/annurev-neuro-080317-062245

Rushton, S. K., Harris, J. M., Lloyd, M. R., & Wann, J. P. (1998). Guidance of locomotion on foot uses perceived target location rather than optic flow. *Current Biology : CB*, *8*(21), 1191–1194. https://doi.org/10.1016/s0960-9822(07)00492-7

Selgrade, B. P., Toney, M. E., & Chang, Y. H. (2017). Two biomechanical strategies for locomotor adaptation to split-belt treadmill walking in subjects with and without transtibial amputation. *Journal of Biomechanics*, *53*, 136–143. https://doi.org/10.1016/j.jbiomech.2017.01.012

Shannon, C. E. (1948). A Mathematical Theory of Communication. *Bell System Technical Journal*, *27*(3), 379–423. https://doi.org/10.1002/j.1538-7305.1948.tb01338.x

Shorten, H. R., Valiant, G. A., & Cooper, L. B. (1986). FREQUENCY ANALYSIS OF THE EFFECTS OF SHOE CUSHIONING ON DYNAMIC SHOCK IN RUNNING. *Medicine & Science in Sports & Exercise*. https://doi.org/10.1249/00005768-198604001-00398

Smith, J. D., & Martin, P. E. (2007). Walking patterns change rapidly following asymmetrical lower extremity loading. *Human Movement Science*, *26*(3), 412–425. https://doi.org/10.1016/j.humov.2006.12.001

Snyder, L. H., & King, W. M. (1996). Behavior and physiology of the macaque vestibulo-ocular reflex response to sudden off-axis rotation: Computing eye translation. *Brain Research Bulletin*, *40*(5–6), 293–301. https://doi.org/10.1016/0361-9230(96)00118-9

Torres-Oviedo, G., & Bastian, A. J. (2010). Seeing is believing: Effects of visual contextual cues on learning and transfer of locomotor adaptation. *Journal of Neuroscience*, *30*(50), 17015–17022. https://doi.org/10.1523/JNEUROSCI.4205-10.2010

Torres-Oviedo, G., Vasudevan, E., Malone, L., & Bastian, A. J. (2011). Locomotor adaptation. In *Progress in Brain Research* (Vol. 191, pp. 65–74). Elsevier B.V. https://doi.org/10.1016/B978-0-444-53752-

2.00013-8

Tresilian, J. (2012). Sensorimotor control and learning: An introduction to the behavioral neuroscience of action. In *Sensorimotor control and learning: An introduction to the behavioral neuroscience of action.*

Turvey, M. T. (1990). Coordination. *American Psychologist*, *45*(8), 938–953. https://doi.org/10.1037/0003-066X.45.8.938

Vasudevan, E. V. L., Torres-Oviedo, G., Morton, S. M., Yang, J. F., & Bastian, A. J. (2011). Younger is not always better: Development of locomotor adaptation from childhood to adulthood. *Journal of Neuroscience*, *31*(8), 3055–3065. https://doi.org/10.1523/JNEUROSCI.5781-10.2011

Warren, J., Kay, B. A., Zosh, W. D., Duchon, A. P., & Sahuc, S. (2001). Optic flow is used to control human walking. *Nature Neuroscience*, *4*(2), 213–216. https://doi.org/10.1038/84054

Warren, W. H. (1990). The Perception-Action Coupling. In *Sensory-Motor Organizations and Development in Infancy and Early Childhood* (pp. 23–37). Springer Netherlands. https://doi.org/10.1007/978-94-009-2071-2_2

Wilson, V. J., Boyle, R., Fukushima, K., Rose, P. K., Shinoda, Y., Sugiuchi, Y., & Uchino, Y. (n.d.). The vestibulocollic reflex. *Journal of Vestibular Research : Equilibrium & Orientation*, *5*(3), 147–170. Retrieved December 20, 2019, from http://www.ncbi.nlm.nih.gov/pubmed/7627376

Winter, D. A. (1983). Moments of force and mechanical power in jogging. *Journal of Biomechanics*, *16*(1), 91–97. https://doi.org/10.1016/0021-9290(83)90050-7